Master thesis

Nudging the Arctic Ocean to quantify Arctic sea ice feedbacks

Evelien Dekker

Universiteit Utrecht

Meteorology, Physical Oceanography and Climate
Marine Sciences

Supervision

Koninklijk Nederlands
Meteorologisch Instituut
Ministerie van Infrastructuur en Milieu

Royal Netherlands Meteorological Institute
Richard Bintanja
Camiel Severijns

Utrecht University, Institute for Marine and Atmospheric Research
Willem Jan van de Berg
Utrecht University, Marine Sciences
Francesca Sangiorgi

Abstract

With Arctic sea ice potentially melting away halfway through this century, the sea ice surface albedo and insulating effect in the Arctic significantly will decrease considerably. The ongoing Arctic sea ice retreat also has an influence on the strength of the Planck, lapse-rate, cloud and surface albedo feedbacks, as well as on the heat exchange between the ocean and the atmosphere, but their combined effects on climate sensitivity has not been quantified. This study presents the first estimate of all Arctic sea ice related climate feedbacks combined, including the nonlinear interactions between the atmospheric feedbacks.

To do so, we use a novel method to keep Arctic sea ice at its present-day distribution under a changing climate. We use a global climate model (EC-Earth V2.3) in which we adapt and apply the nudging procedure to the Arctic Ocean. The sea ice is kept close to its present-day distribution by nudging the Arctic Ocean to its present-day mean temperature and minimum salinity below the present-day Arctic sea ice cover.

We use this nudging method in 50-year simulations in which we applied instantaneously forced 1.5xCO_2, 2xCO_2 and 4xCO_2 radiative forcing. As a result, we are able to preserve about 95% present-day mean March Arctic sea ice area over the last 25 years of all simulations. The summer sea ice cover is less well preserved — 80%, 64% and 32% of the present-day September sea ice area is maintained in the nudged 1.5xCO_2, 2xCO_2 and 4xCO_2 simulations respectively.

The required annual mean nudge energy correction to keep the Arctic Ocean at its present-day mean temperature state in the last year of integration is -0.44, -0.67 and -1.31 $W\ m^{-2}$ for the nudged 1.5xCO_2, 2xCO_2 and 4xCO_2 simulations respectively, which is relatively small compared to the respective greenhouse forcings. The order of magnitude of this correction energy flux is similar to other studies that attempt to force Arctic sea ice into a present-day state starting from warmer future climate. Taking into account our energy correction as response of the climate system, our best estimate of the Arctic sea ice feedback yields of 0.68 $\pm$ 0.16 $W\ m^{-2}\ K^{-1}$, obtained from the CO_2-doubling simulation.

Contents

1 Introduction

The Arctic is one of the regions most affected by climate change (Collins et al., 2013). Observations and modeling studies show that in the Arctic, temperature changes 2 to 3 times faster than the global mean (Holland and Bitz, 2003; Serreze and Barry, 2011). This phenomenon, called Arctic amplification, is driven by climate feedbacks, in which sea ice seems to play a crucial role (Screen and Simmonds, 2010). Feedbacks are processes in the climate system that oppose or amplify the climate response to an external perturbation, like an increase in greenhouse gases. "Any process that responds to temperature change and directly or indirectly affects the radiative balance may be considered as a feedback" (Crook et al., 2011). The net effect all climate feedbacks equals the climate sensitivity. Sea ice is the primary driver of Arctic variability and change (Van der Linden et al., 2014). Therefore, sea ice related feedbacks are a key component of Arctic climate change.

The net effect of the sea ice related feedbacks in the Arctic is not well known. Models are very uncertain regarding the projected warming as they simulate Arctic temperature increases ranging from 5.2 up to 11.4 $^{\circ}$ Celsius in 2081–2100 using the business as usual scenario RCP 8.5 (Collins et al., 2013). Furthermore, not all climate models simulate the present-day (PD) and historic sea ice state equally well (Van der Linden et al., 2014). Also, models differ widely as to when Arctic summer will become sea ice free (Collins et al., 2013). A further complication is that sea ice related climate feedbacks are not constant in time, as they depend on the state of the climate (Andry et al., 2017). The inter-model spread in projected sea ice changes can be linked mainly to differences in sea ice related parameterizations between the models. These differences cause the strength of sea ice feedbacks to vary among the climate models. In this way, the Arctic sea ice contributes differently to the current climate sensitivity in the various climate models. These considerable differences among climate models concerning the PD sea ice state, its variability and the sea ice feedbacks all contribute to the large spread in future projections of Arctic sea ice and Arctic amplification.

The equilibrium global mean climate sensitivity, being the temperature response to a doubling of atmospheric CO_2 and determined by climate models as part of the Coupled Model Intercomparison Project phase 5 (Taylor et al. (2012), CMIP5) ranges from 2.1 to 4.7 K (Andrews et al., 2012). These considerable intermodel differences in global mean climate sensitivity are governed by uncertainties in the various feedback processes, as discussed above, which globally are mainly associated with clouds. In the Arctic, changes in sea ice cover impact cloud and evaporation feedbacks (Colman et al., 1997), but also governs changes in surface reflectivity (albedo) and in ocean-atmosphere heat fluxes.

With sea-ice potentially disappearing sometime during this century ,at least in summer (Snape and Forster, 2014), sea ice related climate feedbacks will become substantially weaker once all sea ice has disappeared. Moreover, the disappearance of sea ice has large implications for society. An ice-free Arctic facilitates increased economic activities like fishery, transport and tourism, potentially leading to ecological damage and pollution with severe consequences for local communities and the Arctic environment. Changes Arctic in sea ice potentially have a more widespread impacts on climate (Overland et al., 2016), such as altering climate extremes in the northern hemisphere midlatitudes. Hence it is vital to assess the reasons for the strong climate changes in the Arctic and to quantify the associated regional feedbacks. To better understand climate it is thus essential to understand what the total climate feedback would be without Arctic (September) sea ice. However, climate feedback parameters are hard to quantify, mainly because feedbacks interact with each other.

A feedback is defined as the temperature change caused by a particular process that invokes a radiative forcing. Many studies have been devoted to understanding the processes behind climate feedbacks and to estimate their strength and contribution to Arctic amplification (Hansen et al., 1984; Bintanja and Oerlemans, 1995; Gregory et al., 2004; Hall, 2004; Bony et al., 2006; Soden et al., 2008; Graversen and Wang, 2009; Crook et al., 2011; Block and Mauritsen, 2013; Mauritsen et al., 2013; Crook and Forster, 2014; Graversen et al., 2014; Pithan and Mauritsen, 2014; Chung and Soden, 2015). Several methods can be applied to quantify climate feedbacks. The climate

feedback strength can be obtained by evaluating the differences in the global mean top of the atmosphere (TOA) net radiation and the differences between global mean surface temperature of two equilibrium climate states, for instance the PD climate and a $2xCO_2$ climate.

The strength of feedbacks can also be calculated without the necessity of long model simulations to reach equilibrium, by using a linear regression method (Gregory et al., 2004). This method allows one to quantify the climate sensitivity from a regression of the global mean TOA radiation imbalance change against global mean surface air temperature change, assuming that this relation is approximately linear and assuming that the radiative forcing is constant in time. This regression method separates the changes of climate state variables (temperature, albedo and water vapor) into a linear and non-linear part and assumes that the feedbacks are linearly additive for small radiative forcings. This method thus assumes that feedbacks do not amplify each other and that nonlinear responses are considered as rapid adjustments (Chung and Soden, 2015).

Another method, the finite differencing or Kernel method - (Soden et al., 2008) takes these rapid adjustments into account. This method allows one to define a variable dependent feedback function (Kernel) in space and time, that describes the unit perturbation of a certain climate variable for a given feedback. Using this method, a unit perturbation of a certain field (eg. temperature, albedo, water-vapor) is related to a perturbation of net clear-sky radiation at TOA through a so-called Kernel. The classical way to assess feedbacks is to artificially suppress certain processes online (hence during a model integration). This has been done for instance to quantify the surface albedo feedback (Hall, 2004; Mauritsen et al., 2013; Graversen et al., 2014).

In this study, we attempt to quantify what fraction of the current climate sensitivity is associated with changes in Arctic sea ice. We therefore aim to separate all climate feedbacks related to Arctic sea ice from the rest. Locking different processes like albedo, lapse rate, or water vapor separately, is not helpful to study Arctic sea ice only feedbacks, because "the surface albedo and lapse rate feedback interact considerably at high latitudes to the extent that they cannot be considered independent feedback mechanisms on global scale" (Graversen et al., 2014).

A negative trend in Arctic sea ice will invoke a cascade of feedback processes in the Arctic that also will have consequences for climate globally. Our main aim is to quantify the net effect of this cascade of processes related to Arctic sea ice retreat, on the global mean surface air temperature and on the net imbalance at TOA. In this study we will use the state-of-the-art climate model EC-Earth (Hazeleger et al., 2012); we will apply a novel method to keep Arctic sea ice at its PD distribution under a changing climate.

We perform model two sets of simulations in which we instantaneously increase the CO_2 concentration. In the first set, we apply just instantaneous CO_2 forcing as usual. In the second set, we we will apply the novel technique to keep sea ice at present-day (PD) distribution. We then compare the feedback estimates resulting from both simulations. In this way we can make an estimate of the (combined) feedbacks associated with Arctic sea. This comparison thus allows us to quantify the part of the response caused by sea ice processes, and thus the overall Arctic sea ice related feedback, including surface albedo and insulation effect (clouds, lapse rate and water vapor).

2 Theory

In this section we will give a brief overview of the processes governing sea ice growth and melt. This will provide the necessary "sea ice background" to explain the adaptations implemented in the model to preserve present-day sea ice. Next, we describe the relevant feedback processes an their relation to sea ice. We conclude this chapter by a discussion of the issue of separating the sea ice only feedback from the total climate feedback parameter.

2.1 The processes governing sea ice growth or melt

Melt or growth of sea ice is governed by the energy fluxes to and from the ocean surface or sea ice (i.e. the surface energy balance). The total energy balance is made up of heat fluxes from the ocean, the atmosphere and the conductive heat flux through the ice. The conductive heat flux depends on the sea ice thickness and the presence of snow on top of the ice. The net heat

flux from the atmosphere to the sea ice depends among others on the ice albedo, cloudiness and temperature difference between the ice and the atmosphere. The heat flux from the ocean to the ice depends on the ocean temperature and salinity stratification. In summary, the net energy balance of sea ice depends on the states of the sea ice, of the ocean and the atmosphere and their mutual interaction. The relative importance of the various energy fluxeson the total heat balance of the ice depends strongly on the season.

The Arctic climate is characterized by a very strong seasonal cycle due to the polar night and day. The cooling of surface water starts in October, when the suns disappears and the polar night begins. The Arctic sea ice extent and thickness increases until the sun reappears again in March. The energy from the sun is consequently used to melt the ice, and once it has disappeared, to warm the ocean. The seasonal sea ice cycle in the Arctic is characterized by the minimum ice extent in September and the maximum ice extent in March.

Growth The strength of the upper ocean stratification governs the water column depth that needs to be cooled before sea ice can grow. The mixed layer properties (e.g. stratification) therefore affect how long it takes to cool down to freezing point. This is because during the process of surface cooling, cooled denser surface water sinks and subsequent convection replaces the cooled water with lighter, warmer water until the entire mixed layer has a uniform temperature. Whether the open ocean actually reaches freezing point depends on how much heat is lost in the form of the heat and moisture fluxes at the ocean-air interface as well as the ocean hat influx from lower latitudes.

Melt The onset of melt occurs if the net heat flux into the ice is negative and if the ice is at its melting point. Sea ice retreat refers to a definite loss of sea ice cover, so when ice has melted away in summer and does not grow back in consecutive years. Melt from the top of the ice pack invokes the formation of melt ponds that cause a drastic reduction in surface albedo, thereby further amplifying the sea ice melt. When ice melts from the bottom, the melt water accumulates in a relatively thin layer of fresh water at the top of the water column, strengthening the ocean stratification. A strong stratification may prevent the sea ice bottom to come into contact with relatively warm ocean water deeper down. Melt and growth can also occur laterally which is influenced by the ocean waves.

Influence of winds and currents The wind field plays an important role in the movement of sea ice, thereby controlling a considerable part of the net Arctic ice loss by exporting ice to subarctic seas where higher temperatures cause rapid melt. Ridging refers to the process of convergence of sea ice, leading to packing and thus thickening of the sea ice. Ridging is the main source of multi-year sea ice, which is ice that is thick enough to survive the melt season. Storms can break up a thin ice pack, causing the formation of open water sites (leads) inside the sea ice pack.

Lead formation can (temporarily) disturb the stable stratification of the Arctic atmospheric boundary layer. An opening in the sea ice cover can generate enormous turbulent heat releases from the ocean to the air and locally this gives rise to cloud formation.

Finally, the wind pattern and ocean currents facilitate transport of ice, out of the Arctic basin. For example, 10–18 % of the sea ice in the Arctic Ocean is annually exported through Fram Strait. According to CMIP5 simulations over the period of 1957–2005, this export accounts for up to 35% of the year-to-year Arctic sea ice interannual variability (Langehaug et al., 2013).

2.2 Climate sensitivity and climate feedbacks

The main aim of this study is to understand how the climate changes in the future, and specifically the role of Arctic sea ice retreat herein. In order to do so we can study the climate response to a perturbation such as an increase in CO_2 concentration in the atmosphere. The global mean surface, T_s is a widely used proxy to describe the mean climate state. This proxy is commonly used because the spatial and seasonal patterns of change in many variables scale quite well with ΔT_s.

The way climate responds to a perturbation can be studied in climate model simulations. Climate sensitivity is a measure of how much global mean surface temperature change occurs response to a certain radiative forcing. The equilibrium climate sensitivity is defined as the global

mean surface temperature change after the climate system has settled in a new equilibrium state in response to a doubling of CO_2 concentration in the atmosphere.

A CO_2 perturbation has an indirect effect on the atmospheric temperature. Namely, an atmosphere with an increased greenhouse gas concentration will have a lower emissivity of long wave radiation. Because greenhouse gases absorb (and emit) longwave radiation.

Therefore, an increase in CO_2 levels will cause an imbalance of incoming shortwave ad outing longwave at the TOA. The established net radiation imbalance at the TOA due to CO_2 is referred as the forcing ΔQ. It leads to a net gain of heat in the atmosphere and ocean, and as a result to an increase of the temperature of the atmosphere and the ocean surface. An increase in the atmospheric temperature invokes a cascade of effects on processes involving temperature and other climate variables. The net effect of this cascade of processes on global mean surface temperature comprises the total climate feedback.

The initial imbalance at TOA (ΔQ) will change over time due to various processes in the climate system that seek to restore the TOA radiative balance. The actual imbalance at TOA in a transient climate (a climate that is out of equilibrium) is defined as ΔR. Ideally we can compare two equilibrium climate states: the equilibrium state before the CO_2 perturbation is applied, and the state after the new equilibrium is reached. The way to study feedbacks is to pose ΔR, the radiative imbalance at TOA , as a function including the initial forcing term ΔQ and a temperature dependent feedback term.

$$\Delta R = \Delta Q + \lambda_f \Delta T_s \tag{1}$$

Here Δ refers to the difference between the two compared equilibrium climate states and λ_f denotes the total climate feedback parameter in $Wm^{-2}\ K^{-1}$. After perturbing the equilibrium climate with a certain initial forcing ΔQ, the climate will slowly settles into to a new mean climate state, in which $\Delta R = 0\ W\ m^{-2}$ again. This new mean climate state will have a new global mean equilibrium temperature different from the initial state. We can use equation 1 to compute the equilibrium temperature change associated with the forcing ΔQ by:

$$\Delta T_s = -\frac{1}{\lambda_f}\Delta Q \tag{2}$$

This theoretical framework allows one to compute the temperature response to a certain forcing where the climate feedback parameter represents all processes in the climate system.

Decomposition of the climate feedback parameter The total climate feedback contains contributions of many processes. Therefore, the total climate feedback λ_f is expressed as a number of separate processes,

$$\lambda_f = \lambda_0 + \lambda_\Gamma + \lambda_w + \lambda_c + \lambda_\alpha \tag{3}$$

Rising surface temperatures lead to an increase in outgoing longwave radiation. This strong negative feedback is called the Planck feedback (λ_0). Secondly, the temperature increase generally does not occur vertically uniform throughout the troposphere, which gives rise to the so-called lapse-rate (λ_Γ) feedback. Thirdly, the water vapor feedback describes that warmer air can hold more water vapor, which is a strong greenhouse gas in itself. More evaporation can enhance the formation of clouds. Clouds affect both the reflection of shortwave radiation and the emission of longwave radiation. The net temperature effect clouds is called the cloud feedback (λ_c). Finally, increasing temperatures lead to the melt of ice and snow, which will lead to a reduction of the reflection of shortwave radiation. This enhances further warming in a process called the surface albedo feedback (λ_α).

The strength and relative importance of all these separate processes is not uniformly distributed over space and season. As a consequence, the temperature increase in response to a radiation perturbation varies strongly in space and time.

2.3 Feedback processes related to Arctic sea ice

The Arctic is a region very sensitive to climate change. This extreme sensitivity can be inferred from the recent increased variability of sea ice extent as recorded by satellites(Serreze and Stroeve,

2015). This is for a large part explained by many feedback processes in the Arctic (Screen and Simmonds, 2010). Specifically, processes related to sea ice are involved in the above mentioned feedbacks. The retreat of Arctic sea ice directly influences the radiative balance at the surface as well as the surface temperature, affecting a number of other feedback processes.

In addition, the retreat of Arctic sea ice also has an impact on processes on the global scale that are not directly related to the local radiative balance. We will also identify processes that describe the interaction with climate outside the Arctic, which can be regarded as indirect feedback processes. In the following sections we will discuss the processes that are involved in direct and indirect feedbacks.

2.3.1 Direct feedbacks

Local retreat in sea ice cover influences the local radiative balance and surface temperature in three distinct ways: 1) reduction of highly reflective ice cover which is related to the albedo feedback, 2) removal of the sea ice that insulates the ocean from the atmosphere and 3) fresh water originating from melting sea ice affects the density stratification of the ocean.

Insulation feedback The removal of the insulating ice layer, causes an enhanced rate of heat and moisture exchange between the ocean and the atmosphere. When sea ice cover is replaced by open water, the seasonal cycle in ocean heat storage is altered dramatically.

Additional radiation will be taken up by the ocean in the spring and summer seasons and stored in the ocean. In winter, this extra ocean heat can easily be released to the atmosphere by means of turbulent heat fluxes when sea ice is absent. Also, the increase of open water area will enhance evaporation and subsequently the water vapor content in the atmosphere as well as cloud formation. Sea ice retreat thus modulates the water vapor and cloud feedbacks, and also interacts with the lapse rate feedback by altering the vertical temperature gradient in the lower atmosphere.

Ice-ocean feedback The growth of sea ice in winter causes salt to mix to deeper layers. The melt of sea ice causes a net freshwater flux, which stays in a shallow layer at the surface. The seasonal cycle of sea ice thus results a net vertical transport of salt, which leads to a more stable water column (Goosse and Zunz, 2014). As a consequence of this stable stratification, heat from deeper ocean water cannot reach the sea ice. This is a positive feedback processes.

2.3.2 Indirect processes & feedbacks

Ocean advection feedback Melting of sea ice Arctic causes a freshwater flux into the Arctic Ocean. Significant freshwater perturbations potentially have an effect on the strength of the meridional overturning circulation (MOC) (Stommel, 1961; Marotzke, 2000). The so-called salinity advection feedback originates from the warm and relatively salty water that is transported towards higher latitudes in the North Atlantic. This salt water cools and sinks and is exported southward at depth. If the Atlantic part of the Arctic ocean becomes too fresh (due to increased ice melt, precipitation and river run-off), the strength of the AMOC strength could decline. The resulting reduced heat and salt transport into the Arctic basin can act as a negative, stabilizing feedback on sea ice melt. However, studies have shown that is is hard to predict the nature and sign of the net ocean advection feedback (Council et al., 2004).

Wind stress vulnerability A more general effect of sea ice retreat or thinning is that the remaining ice will become more vulnerable to heat flux perturbations and wind stress. Andry et al. (2017) found that apparently there exists a certain threshold in sea ice thickness for which Arctic sea ice reduction shifts from being dominated by thinning, to being dominated by areal shrinking. Feedbacks are also enhanced by remote processes. With climate change, winds in the Arctic may change, which has a effect on wind-stress and also on the moisture transport into the Arctic.

2.4 Separation of the Arctic sea ice feedback

Feedbacks that directly relate changes in the net TOA imbalance to surface temperature increase are commonly decomposed into the Planck feedback (λ_0), the lapse-rate feedback (λ_Γ), the

water-vapor feedback (λ_w), the surface albedo feedback (λ_α) and the cloud feedback (λ_c). Mathematically, this boils down to writing equation 2, which assigns the surface temperature changes in response to a forcing ΔQ changes to specific feedback processes as:

$$\Delta T_s = -\frac{\Delta Q}{\lambda_0 + \lambda_\Gamma + \lambda_w + \lambda_c + \lambda_\alpha} \tag{4}$$

The feedback strength related to Arctic sea ice only, consist of the direct feedback associated with Planck, albedo, lapse-rate ands clouds, but also of the combined indirect feedbacks. Each of these individual feedbacks has a sea ice related component. However, we are unable to split the Arctic sea ice part of these processes (as in equation 4) from the non-sea ice part. Hence, we will take another approach.

Like in most feedback studies, we assume that temperature response to a perturbation linearly can be decomposed into various feedbacks, and one can choose the specifics of the decomposition. Hence, we can write the feedback parameter decomposition in any way we like:

$$\lambda_f = \sum_{i=0}^{N} \lambda_i \tag{5}$$

As we want to know the Arctic sea ice only part of the total feedback, we split this into two parts: one related to Arctic sea ice and one unrelated to sea ice.

$$\lambda_f = \lambda_{ice} + \sum_{i=1}^{N} \lambda_i = \lambda_{ice} + \lambda_{rest} \tag{6}$$

where subscript "ice" denoted the Arctic sea ice part. Hence, the temperature response can also be linearly decomposed. This means that a temperature response solely related to Arctic sea ice can be expressed as:

$$\Delta T_{eq} = \Delta T_{eq}^{ice} + \Delta T_{eq}^{rest} = -\frac{1}{\lambda_{ice} + \lambda_{rest}} \Delta Q \tag{7}$$

As a result we now have framework to describe the sea-ice only feedback λ_{ice}.

2.5 Differences with conventional feedback estimation methods

The separation of the total climate feedback parameter into an Arctic sea ice and a non-Arctic sea ice related part is a novel approach to the authors knowledge. The major advantage of the current technique of estimating the sea-ice feedbacks is that it includes the nonlocal effects, nonlinear and indirect effects of sea ice retreat. This contrasts with the commonly used Kernel method, where the feedback is decomposed into processes that must be directly related to radiative changes at TOA.

The application of kernels to compute the individual climate feedbacks spatial structure reveals the existence of a mismatch between the total climate feedback computed by the Gregory method and sum of the kernel feedbacks (Block and Mauritsen, 2013). They discuss that the Arctic does contributes positively to the climate sensitivity in 4xCO_2 simulations, but that this Arctic contribution is underestimated by the kernel method. Our method allows to quantify the Arctic sea ice climate feedback including the non-linear interaction of the Plank, lapse-rate, cloud and albedo feedback, which is new information to understand the contribution of the Arctic sea ice to the climate sensitivity of the current climate.

3 Methodology

We aim to compute the climate feedback in a regular CO_2 perturbed climate model simulation and in an adapted (nudged Arctic Ocean) climate model simulation, where sea ice is kept as in the initial PD control state under the same CO_2 forcing as in the regular simulation. The climate feedback is calculated using the regression method from (Gregory et al., 2004). This section explains what model we use and the nudging technique. In the last we describe how we derive the Arctic sea-ice only feedback from our data.

3.1 Model

The simulations are carried out using EC-Earth version 2.3. (Hazeleger et al., 2012; Sterl et al., 2012). This is a state of the art, fully coupled global climate model used in CMIP5. EC-Earth's atmosphere component is the Integrated Forecast System (IFS) of the European Center of Medium-range Weather Forecasts (ECMWF) at T159 spectral resolution with 62 levels. EC-Earth's ocean component is represented by the Nucleus for European Modeling of the Ocean (NEMO) (Madec et al., 2008) in the ORCA1 configuration. In this configuration NEMO uses 42 vertical levels and a horizontal resolution of one degree. The sea ice component, dynamic-thermodynamic Louvain la Neuve sea ice model version 2 (LIM2) (Fichefet and Maqueda, 1997; Bouillon et al., 2009), is incorporated in NEMO. The IFS and NEMO component models are coupled using the OASIS3 software (Valcke et al., 2003).

3.1.1 Initial state

All the simulations start from a PD equilibrium state of EC-Earth v2.3 with year 2000 greenhouse gas conditions. This particular state is obtained from the control simulation used in Van der Linden et al. (2014). This control simulation was realized after approximately thousand years with preindustrial (year 1850) forcing and subsequent integration of 44 years with PD forcing. Following these 44 years, the PD control climate of year 2000 was continued for 550 years. We use January 1 2500 of the control simulation as initial state. The control simulation of our study has a length of 60 years.

3.1.2 Model performance in capturing present Arctic sea ice characteristics

The performance of EC-earth in capturing PD climate and Arctic sea ice characteristics was studied in Sterl et al. (2012). In EC-Earth, Arctic sea ice concentration and extent have realistic values compared to observations. However, the sea ice tends to be too thick along the Siberian coast. The mean sea ice transport through Fram strait is in good agreement with available observations. The mean state of Arctic sea ice under preindustrial conditions in 33 CMIP5 models was evaluated in van der Linden (2016) and we can now compare EC-earth to other models sea ice characteristics. Under preindustrial circumstances, EC-Earth simulates the seasonality of sea ice area and volume very low compared to other CMIP5 models. The total Arctic sea ice area is in the very low end of this studies ensemble whereas the total Arctic sea ice volume is relatively high. If a preindustrial EC-earth climate is perturbed with a transient 1% increase of CO_2 over 140 years, EC-Earth shows the highest Arctic 10 year surface air temperature trend of all models. Furthermore, EC-Earth exhibits the second largest sea ice volume decrease trend from this studied ensemble. This means that the Arctic in EC-Earth is very sensitive to CO_2 perturbations, and the results from the simulations performed with EC-Earth might very well differ from other models.

3.2 Nudging the Arctic Ocean to force the sea ice into present-day

We aim to keep the ocean surface temperature and salinity in the PD state, so that Arctic sea ice will also remain close to the PD distribution even in warmer conditions. We anticipate that sea ice growth is still possible under warmer atmospheric conditions if we force the surface waters to be sufficiently fresh and cold. Therefore, we will nudge the Arctic Ocean into a prescribed state obtained from the PD Arctic Ocean in the control simulation. Nudging is a standard technique used in weather and climate models to keep a variable field in or at least close to a prescribed state. The application of nudging only in the Arctic Ocean a new method to keep the Arctic sea ice in its PD distribution under a changing climate.

The nudging method itself affects the climate response to a perturbation, because forcing the Arctic Ocean into a prescribed field yields a subtraction or addition of energy from the climate system. We aim to disturb the climate as little as possible by the nudging method. Therefore, we particularly want to prevent the nudging method itself to directly change the radiation balance at TOA or the surface air temperature.

The only changes in radiation at TOA or surface air temperature should be resulting from the fact that the Arctic sea ice is maintained at its PD distribution. We attempt to accomplish

this by nudging only in the ocean where sea ice is present, because the atmosphere would not be influenced by the changes in the ocean under the sea ice.

Nudging the Arctic Ocean will on the long term have an influence on the temperature in the ocean outside of the Arctic. Therefore, we will only use 50 years of integration to calculate the climate feedbacks. As 50 years is a relatively short timescale in climate analysis, we assume that long term ocean climate feedbacks are of no significance for the Arctic sea ice related climate feedback.

3.2.1 Implementation of the nudging procedure in the ocean model

The standard nudging routine in NEMO is implemented in the routine $tradmp.F90$, more detailed explanations can be found in the NEMO handbook of Madec et al. (2008). Nudging boils down to adding an extra damping term to the state variable equation of interest. In case of tracer damping of temperature and salinity in an arbitrary grid-cell and time step this amounts to:

$$\frac{\partial T}{\partial t} = ... - \gamma(T - T_0), \frac{\partial S}{\partial t} = ... - \gamma(S - S_0) \tag{8}$$

Here γ denotes the inverse time scale of damping. The model temperature and salinity are represented by T an S and T_0 and S_0 represent the climatological values that we want to prescribe. The combination of where, how strong and towards what fields we nudge is explained below. The optimal combination of parameters that was found after testing many different combinations of γ, T_0 and S_0. The criterion we used is that the nudging procedure should keep the sea ice area close to the control simulation area during the first 10 year test runs. Most important, the PD sea ice should not become less than the minimum sea ice area in the control simulation. The combination of parameters that is used to perform the simulations of the experiments is described below. A full overview of all test simulations and the results are described in the in the appendix A.

3.2.2 Choice of target field

In the nudged simulations, the Arctic Ocean temperature and salinity fields will be damped towards prescribed monthly climatology fields. We prescribe monthly climatology fields of ocean salinity and temperature obtained from a PD equilibrium control simulation of 60 years.

Temperature target field The ocean temperature field is nudged towards the monthly mean climatology of the 60 year PD control run. Ideally, this means that if we apply this nudging to the control simulation itself, nudging itself on will on average not lead to an energy loss or gain of the ocean (not tested). We expect a global mean increase in ocean temperature after perturbing the climate with CO_2, so that the applied nudging will lead to a cooling of the Arctic ocean. By quantifying the energy loss due to the nudging, we can take this term into account when we calculate the sea ice feedback. The energy tendency associated with the nudging of temperature is

$$\frac{\partial E_{nudge}}{\partial t}|_{ijkt} = -\gamma_{i,j,k}(T - T_0)_{i,j,k,t} * V_{i,j,k} * C_p * \rho_0 \tag{9}$$

where C_p is the heat capacity of sea water [$J\ kg^{-1}\ K^{-1}$], V is the volume of the cell [m^3] and ρ_0 is the density of seawater [$kg\ m^{-2}$]. This quantity is calculated in each grid cell and for every time step during the model integration.

The RCP scenario simulation carried out with EC-Earth reveal a dominant role of the ocean heat supply from the Atlantic into the Barents Sea with respect to the Arctic sea ice retreat (Koenigk et al., 2013). We anticipate that the role of the ocean in facilitating northward heat transport into the Arctic basin is suppressed when we apply the nudging technique. In the Barents Sea among other regions, the ocean heat content plays a dominant role in sea ice variability (Smedsrud et al., 2013; Årthun et al., 2012; van der Linden et al., 2017; Li et al., 2017). The nudging method aims to maintain sea ice near the PD configuration, especially in the regions where the ocean plays an important role.

Salinity target field The ocean salinity field is nudged towards the monthly climatology of the minimum salinity values over the 60-year PD control simulation. As a consequence, applying the nudging to the control simulation will lead to a anomalously fresh Arctic ocean column. Restoring the Arctic ocean towards salinity minimum climatology instead of salinity mean climatology turned out to be the essential part of the method that enables us to maintain the sea ice close to PD. In all test runs in which we nudged towards a monthly mean ocean salinity climatology, the sea ice drifted away from its PD state.

It is not straightforward to quantify the dynamical energy loss or gain from adjusting the salt content. Adapting the salt budget potentially has consequences for the strength of the density driven currents in the Arctic Ocean and the Atlantic meridional overturning circulation. However, quantifying the density change effect of the nudging procedure is not part of this thesis. We expect that in terms of ocean energy budget, the Arctic ocean heat content change due to temperature nudging has a larger effect on the local energy budget than the dynamical energy change caused by nudging the salt content. We expect that nudging the salt content has no direct consequences for the heat exchange with the atmosphere. This is also an important motivation to nudge in the ocean to maintain sea ice.

3.2.3 Construction of the 3D nudge mask

Nudging the Arctic Ocean to maintain the sea ice is only required in locations where sea ice can form. For this reason, a mask is constructed to ensure the high latitude ocean is nudged in suitable locations. From the 60 year control PD simulation, we compute the monthly climatology of the sea ice concentration. The resulting climatology is used to construct the mask. All grid cells that ever had nonzero sea ice concentration in the Northern Hemisphere during the entire control simulation are filled with ones, the remaining cells are filled with zeros. In this way we obtain a monthly nudge mask, so for each month (Jan-Dec) we have a unique nudge mask. This mask is used to construct a three-dimensional nudge field, which represents γ in equation 8.

The vertical structure of the nudge field is set up according to two different versions (the version numbering is explained in Appendix A).

Mixed layer In version 49, we nudge only the mixed layer, where only the upper 17 ocean layers in NEMO, i.e. the upper 200 meters are nudged. In this way we anticipate that the mixed layer temperature and salinity are of importance for sea ice formation, whereas deeper layers have much less influence on the sea ice. By not nudging the deep layers, we have to extract less energy from the system, thereby disturbing climate to a lesser extent.

Entire column In version 50 we nudge the entire column towards the PD state, so as to prevent the potential occurrence of unrealistic convection. This unrealistic convection might occur when the temperature in the mixed layer is nudged down so much, meaning that the near-surface density becomes higher than the density of the deeper layers.

The value of the timescale of damping, γ, obtained after the test simulations was $20^{-}1$ day. This damping has a timescale of almost one hour, which is a very strong form of nudging.

3.2.4 Simulations

We analyse one control run of 60 years long in which the greenhouse gas forcing remains as in PD. Furthermore, we carried out three instantaneous CO_2 forcing experiments, namely 1.5xCO_2, 2xCO_2 and 4xCO_2, 50 years long. Along with these CO_2 simulations, we performed similar CO_2 but with both nudging methods (nudge version for mixed layer only, and for the entire column) active. However, it turned out that the strong nudging routine can cause the ocean to become unstable, thereby crashing the simulations. For this reason, only three out of the six planned nudged nudged simulations could be carried on for 50 years. This is a result presented in appendix A. The seven analyzed simulation are summarized in table 1.

Table 1: Simulations

Simulation name	CO_2	ppmv	nudging	length (years)
control	PD	368.9	-	60
1.5xCO_2	1.5x PD	535.3	-	50
nudge 1.5xCO_2_49	1.5x PD	535.3	mixed layer upper 17 levels (200 m)	50
2xCO_2	2x PD	737.7	-	50
nudge 2xCO_2_50	2x PD	737.7	all 42 levels (>5000 m)	50
4xCO_2	4x PD	1475.5	-	50
nudge 4xCO_2_50	4x PD	1475.5	all 42 levels (>5000 m)	50

3.3 Calculation of climate feedbacks

The six CO_2 forced simulations (subsection 3.2.4) provide output of monthly mean net TOA radiation and surface temperature. The nudged simulations also output the nudge energy due to temperature damping. As described in the theory section, computation of the climate feedback is done by comparing two equilibrium states (before and after perturbation). We evaluate the total energy imbalance against the global mean temperature response. As we aim to calculate the Arctic sea ice related feedback, we split the response in a Arctic sea ice related part (subscript ice) and the non Arctic sea ice related part.

$$\Delta T_{eq} = \Delta T_{eq}^{ice} + \Delta T_{eq}^{rest} = -\frac{1}{\lambda_{ice} + \lambda_{rest}} \Delta Q \tag{10}$$

The regular CO_2 simulations and the nudged CO_2 simulations provide required output to compute the Arctic sea-ice only feedback. This section explains how we do this.

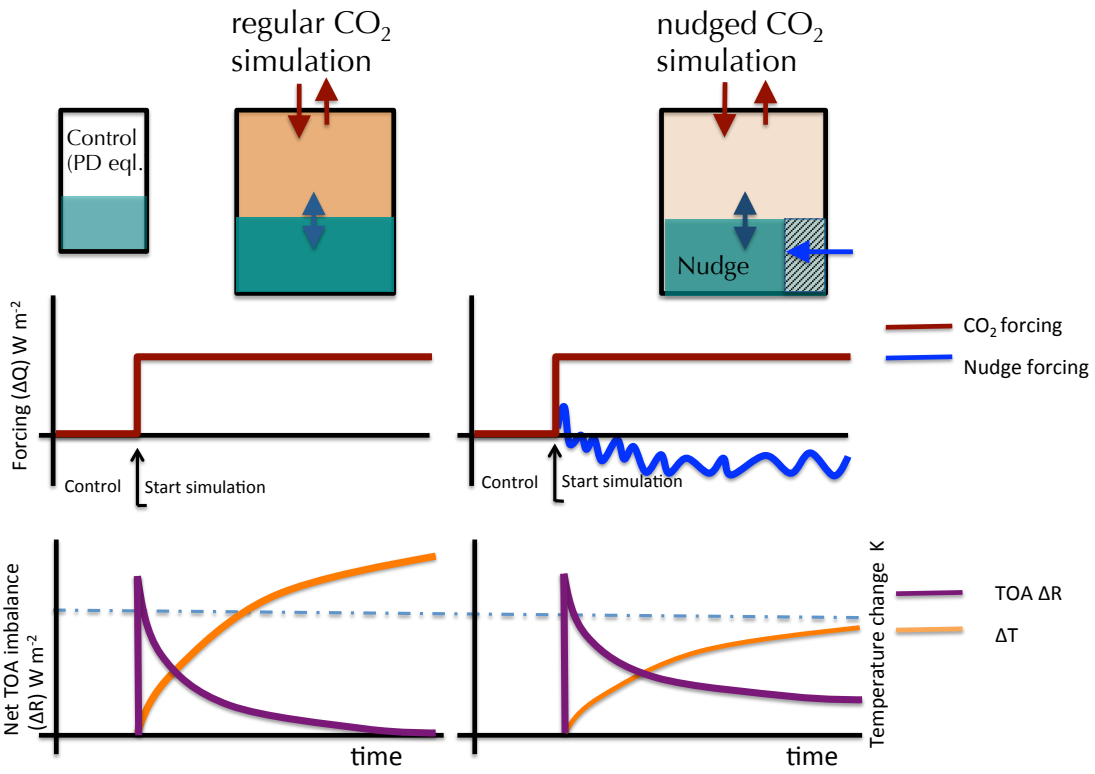

Figure 1: Illustration of the simulation set-up. Top row: forcing applied in the two simulations. Bottom row: climate system response to the forcing. Left: expected forcing and response in the regular CO_2 simulation. Right: The expected forcing and response in the adapted nudged CO_2 simulation.

In Figure 1, the expected response of net TOA radiation and global mean surface air temperature to the applied CO_2 forcing and nudging is schematically illustrated for both (regular and nudged) simulations. The CO_2 concentration is increased instantaneously from its PD value at the start of the simulation (red line). The TOA radiative forcing associated with the increase in CO_2 is therefore time and state independent. The forcing associated with the nudging method (blue line) depends on the Arctic Ocean state and is therefore not constant in time. In the regular CO_2 simulation, the net TOA radiation balance will eventually go to zero when the climate system reaches a new equilibrium state. In the nudged CO_2 simulation, the newly established equilibrium is reached when the net TOA imbalance equals the forcing associated with the nudging method. In other words, at some point during integration of the nudged simulations, the energy associated with the nudging will balance the net TOA imbalance. The new climate equilibrium in the nudged simulations is therefore not reached when the net TOA radiation balance is zero, but when the sum of the nudge energy and the TOA imbalance is zero.

3.3.1 Comparing different equilibria

From the two types of simulations (regular and nudged) we aim to obtain the climate feedback parameter. We use the linear regression method of (Gregory et al., 2004) to evaluate λ_f.

In the regular CO_2 simulations we evaluate the slope of linear regression between global annual mean surface air temperature change and top net radiation imbalance change (the difference between the simulation and the control simulation). This regression provides an estimate of the linear dependence of the net TOA radiation imbalance on global mean surface temperature change. Hence, in equilibrium, the linear regression between global mean 2 meter temperature change and

TOA imbalance is represented by:

$$\Delta R^{TOA} = \Delta Q^{\mathrm{CO_2}} + \lambda_f^{\mathrm{CO_2}} \Delta T_{eq}^{\mathrm{CO_2}} = 0 \tag{11}$$

From this regression we obtain ΔQ at $\Delta T = 0$ and ΔT_{eq} at $\Delta R_{TOA} = 0$. Hence, the slope of the regressions from the regular simulations equal the climate feedback λ_f

It is important to realize that the two types simulations do not reach equilibrium in the same way (see Fig. 1). Therefore, evaluating the feedback strength in the nudged simulation using linear regression is less straightforward. In the nudged CO_2 simulations, the climate system is not only forced by an instantaneous CO_2 increase, but also by a time-dependent nudging energy to keep the sea ice near PD distribution. We anticipate that the equilibrium temperature change in the nudged simulation is reached when the TOA imbalance and the nudge energy flux together are zero.

In the regular simulations, the net TOA imbalance changes over time in response to the initial perturbation. On the other hand, in the nudged simulations, the net TOA imbalance as well as the nudge energy changes over time in response to the initial perturbation. Therefore, instead of regressing the net TOA imbalance against global mean 2m temperature change, we regress the sum of the TOA imbalance and the nudge energy against global mean surface temperature change. In this way, we obtain an estimate of ΔQ from applying the nudging and the radiative forcing, and the temperature change that is associated with the balance between the net TOA radiative imbalance and the nudging energy.

Therefore we express the energy balance equation of the nudged CO_2 simulation in equilibrium as follows:

$$\Delta R^{TOA} + \Delta E^{nudge} = \Delta Q^{\mathrm{CO_2}+nudge} + \lambda_f^{\mathrm{CO_2}+nudge} \Delta T_{eq}^{\mathrm{CO_2}+nudge} = 0 \tag{12}$$

3.3.2 Arctic sea ice only feedback

In the regular simulation the climate feedback parameter λ_f includes all feedbacks involved with changes in Arctic sea ice:

$$\lambda_f^{\mathrm{CO_2}} = \lambda_{ice} + \lambda_{rest} = -\frac{\Delta Q^{\mathrm{CO_2}}}{\Delta T_{eq}^{\mathrm{CO_2}}} \tag{13}$$

In the nudged simulation ideally the Arctic sea ice perfectly resembles the PD Arctic sea ice, therefore there are no changes in the global mean temperature and the3 TOA imbalance due to the retreat of Arctic sea ice. Hence, e assume there are no climate feedbacks associated with Arctic sea ice in the nudged simulation, meaning that we can write:

$$\lambda_f^{\mathrm{CO_2}+nudge} = \lambda_{rest} = -\frac{\Delta Q^{\mathrm{CO_2}+nudge}}{\Delta T_{eq}^{\mathrm{CO_2}+nudge}} \tag{14}$$

We evaluate the associated no sea ice feedback by regression of the sum of net TOA imbalance and nudge energy against global mean 2m temperature change.

We now have a way to compute $\lambda_f^{\mathrm{CO_2}}$ and $\lambda_f^{\mathrm{CO_2}+nudge}$. Hence, we can combine these terms to find λ_{ice}, the final goal of this thesis. In order to do so, we must make one important final assumption. We assume that

$$\lambda_f^{\mathrm{CO_2}+nudge} = \lambda_{rest}^{\mathrm{CO_2}} = \lambda_{rest} \tag{15}$$

Physically, this means that processes contributing to the total climate feedback parameter do not change their global mean 2m temperature dependence in the nudged simulations v.s. the regular simulations. This is a critical assumption, because the damping term that causes the energy loss is implemented directly in the $\frac{\partial T}{\partial t}$ temperature evolution equation 8. Hence, the formulation of the climate model, essentially the way climate is represented, is thus fundamentally different in the nudged simulations compared to the regular simulations (but only in the Arctic region). As a consequence, we do not know if the (thermo)dynamics are still comparable, but in order to be able to evaluate the feedbacks, this is a necessary assumption.

Subtraction of eq 14 from eq. 13 yields λ_{ice}:

$$\lambda_{ice} = (\lambda_{rest} + \lambda_{ice})^{\mathrm{CO_2}} - \lambda_{rest}^{\mathrm{CO_2}+nudge} = -\frac{\Delta Q^{\mathrm{CO_2}}}{\Delta T_{eq}^{\mathrm{CO_2}}} - \frac{-\Delta Q^{\mathrm{CO_2}+nudge}}{\Delta T_{eq}^{\mathrm{CO_2}+nudge}} \quad (16)$$

As a result, we subtract the slope estimate of equation 12 from the slope estimate of equation 11 to have an estimate for λ_{ice}.

We are aware that the Gregory method is normally used for evaluating the climate response to a single, time-independent externally applied radiative forcing. Contrastingly, in the climate response in the nudged simulation consists of two distinct forcings of which the nudging forcing is not a external radiative, time and state independent forcing. Therefore, the radiative imbalance due to CO_2 and the applied nudging interact during the transient response of the climate system. Simply put, taking the difference between the slopes of the regular and the nudged simulations as estimated from the Gregory method does for this reason affect the accuracy of this estimate of the Arctic sea ice feedback. Therefore, the use of the Gregory method is questionable.

4 Results

In this chapter we first present the response of the net TOA energy fluxes respond in the nudged and the regular simulations. Then we show how the nudging technique performs. by comparing how the total Northern Hemispheric sea ice evolves during the nudged CO_2-forced simulations. Furthermore we show how the seasonal cycle of sea ice area and volume, and the spatial distribution of the Arctic sea ice to the control state for each CO_2-forced simulation. Then we assess the magnitude of the energy tendency term associated with the nudging of Arctic Ocean temperature. Finally, the Arctic sea-ice related feedbacks are presented and compared to conventional feedback estimates.

4.1 The global annual mean climate response over 50 years

The global annual mean response of the incoming and outgoing energy fluxes of the climate system and related temperature changes are shown in figure 2. The global mean ocean and atmosphere temperatures, the longwave radiation, net TOA radiation and nudge energy flux responses all follow an exponential curve indicating that these variables are adapting towards a new equilibrium state on approximately the same time scale. Generally, the higher the CO_2 perturbation in the simulation, the larger the deviation from the control state. The temperature response ((a) and (b)) of the nudged simulations is lower than in the corresponding regular simulation. In the 1.5xCO_2 simulations the difference in temperature response between regular and nudged is almost negligible.

The initial stage of the simulations is characterized by a sudden decrease in outgoing longwave radiation in comparison with the control simulation (Fig. 2 (c)). This leads to a net long wave radiation gain at the top of the atmosphere, which is most pronounced in the 4xCO_2 simulation. The temperature response is also most pronounced at the start of the simulation (Fig. 2(a)). In the final stage of the simulation, the absolute difference in response between the regular and nudged simulations is largest in the 4xCO_2 simulation and very small in the 1.5xCO_2 simulations.

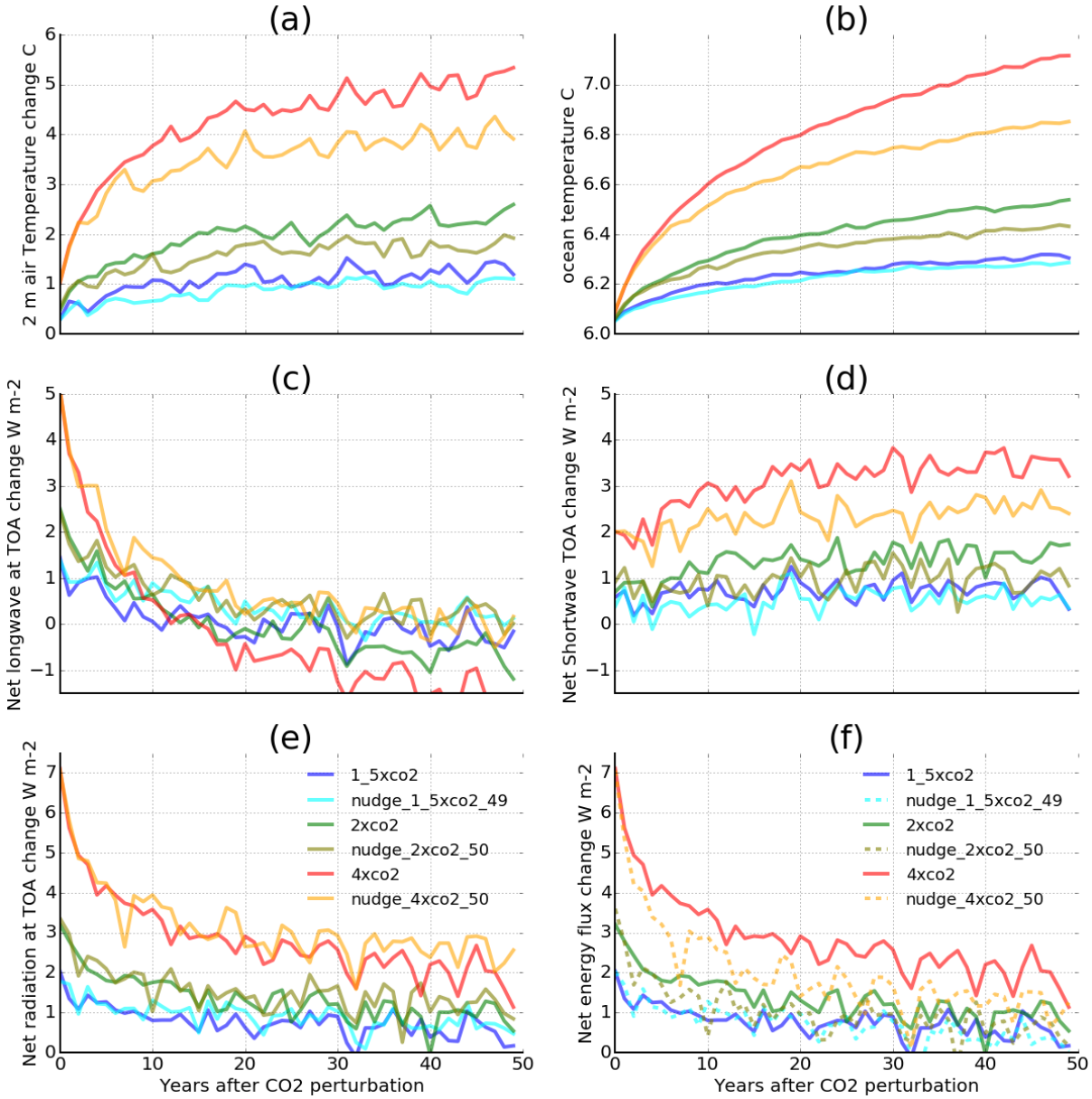

Figure 2: Time series of global annual mean global mean surface temperature change (a), global mean ocean temperature (b), global mean net longwave radiation change (c), global mean net shortwave radiation change (d), global mean net TOA budget change (e) and global mean net energy flux change (net TOA + nudge energy) (f). The nudged simulation total energy imbalance is represented by the nudge energy and TOA radiative imbalance (stippled lines), whereas the regular simulations total imbalance is only made up by the TOA radiative imbalance (solid lines). The global annual mean from the control is subtracted from the global annual mean of the forced simulations to obtain the changes in the energy budgets.

Net TOA response radiation and net energy response The net TOA response is the net change in radiation at the top of the atmosphere. The first year annual mean net TOA change is 7.1, 3.4, 1.8 $W\ m^{-2}$ for the 4, 2 and 1.5xCO_2-forced simulations respectively (Fig. 2(e)). The climate redistributes this energy by increasing the air temperature, ocean temperature and melting of ice. This leads to changes in the longwave outgoing budget and incoming shorwave budget. In all simulations, the net TOA radiation change is initially dominated by the the longwave budget, whereas in the last stage of simulation the net TOA radiation change is dominated by the shortwave radiation budget. As expected, non of the simulations have reached equilibrium 50 years, as the net TOA imbalance is larger than zero. The regular 4xCO_2 simulation is most furthest away from equilibrium as its climate exhibits the largest TOA imbalance after 50 years.

Longwave response The initial longwave response in the regular simulations becomes stronger with higher CO_2 concentrations. In the regular CO_2 simulations, the final net longwave radiation budget is negative compared to the control state. A negative net longwave change budget indicates that more longwave radiation is leaving the Earth's climate system in the new equilibrium state compared to PD. In the CO_2-forced simulations, the incoming shortwave budget has increased compared to PD, because of the planetary albedo loss in response to increased temperatures. In the regular simulations, higher temperatures lead to an increase in longwave outgoing radiation compared to PD.

While the regular CO_2 simulations exhibit a negative final longwave budget change, in the nudged simulations the final longwave radiation budget change approaches zero. This means that within the same time period, a global mean surface temperature rise does not lead to equally proportional net increase of longwave outgoing radiation in the nudged versus regular simulation. The global mean temperature increase in the nudged 4xCO_2 simulation is 4 K, which is four times larger compared to the $\tilde{1}$ K global mean temperature change in the regular 1.5CO_2 simulation. Nevertheless, the net longwave outgoing radiation in the nudged 4xCO_2 is of the same order as the regular 1.5xCO_2 simulation.

This finding suggests that feedback processes other than the Planck feedback have a strong influence on the net longwave radiation in the nudged simulations. This indicates that the temperature damping in the ocean and the sea ice feedback effect have a strong influence on the global mean outgoing longwave radiation budget.

Shortwave response The net incoming shortwave radiative flux alters due to changes surface (ice and snow) and cloud amount and albedo (Fig. 2 (d)). The shortwave response that already occurs in the first year can be related to fast adjustments in cloud amount and albedo (not analyzed). This amounts to 0.6, 1 and 2 $W\ m^{-2}$ for the 1.5, 2 and 4xCO_2-forced simulations respectively. The slow changes in the shortwave budget occur only after the energy gain by CO_2 is used to melt ice and snow, which takes time. In the 4xCO_2 simulations, the shortwave budged change is most evident, as this strong forcing causes the most outspoken decline in ice and snow cover. Despite the nudging routine, the nudged 4xCO_2 simulation still exhibits significant more change in surface and cloud albedo than the regular 1.5 and 2xCO_2 simulations. A more detailed analysis of surface versus cloud albedo is for left for future research.

If we turn the attention to the total energy system imbalance, including the nudge energy loss (Fig. 2(f)), we infer that all nudged simulations seem to converge towards a similar total energy imbalance, whereas the regular simulations seem to diverge more. In the final years of simulation, the energy imbalance due to nudging contributes 50% or even more to the total energy imbalance, meaning that the net TOA imbalance is smaller than the loss due to the nudge energy flux.

4.2 The performance of the nudging technique to maintain PD sea ice

4.2.1 Sea ice time series

In all regular CO_2 simulations the amount of Arctic sea ice area and volume declines shortly after the CO_2 forcing. September Arctic sea ice disappears in the regular simulations 1.5xCO_2, 2xCO_2 and 4xCO_2 in year 13, 8 and 3 respectively (Fig. 3). The disappearance of September sea ice indicates that the surface energy balance in the regular simulations is not compatible with the formation of multi-year sea ice. In the regular 1.5xCO_2 and 2xCO_2 simulations, there is still ice in

March after 50 years after the CO_2 perturbation, as winters are still sufficiently cold.In the 4xCO_2 simulation, winter sea ice area disappears after 40 years. After 25 years, the Arctic sea ice in the regular simulations equilibrates around a new mean state with less sea ice compared to the mean control state.

In the nudged simulations, no clear sea ice retreat trend is in the first 20 years. However, the evolution of absolute difference between the CO_2-forced simulations and the control simulation (Fig. 4) reveals that the nudging does not lead to a sea ice state that is perfectly similar to the control sea ice state.

In the regular simulations, the absolute difference with the control shows a clear difference in summer and winter. Contrastingly, the sea ice difference between the nudged and the control simulations does not exhibit a clear seasonal cycle. Hence, September sea ice at least partly remains in the nudged simulations. Overall, the nudging method does perform less well in maintaining summer sea ice compared to winter sea ice.

Table 2: Sea ice area recovery as fraction of the control PD simulation climatological mean over the last 25 years of integration.

Nudged simulation	March	September
nudge 1.5xCO_2	0.96	0.80
nudge 2xCO_2	0.95	0.64
nudge 4xCO_2	0.92	0.32

4.2.2 The climatological seasonal cycle of the new sea ice state in the final 25 years of simulation

We use the last equilibrated 25 years of the simulations to compute the climatological seasonal cycle of Arctic sea ice area (Fig. 5), volume (Fig. 6) as well as the spatial sea ice distribution in March (Fig. 8) and in September (Fig. 7). In the regular CO_2 simulations, September sea ice has practically disappeared in the last 25 years(figs. 5 and 6 and right panels in Fig. 7). In contrast, in the nudged simulations not all summer sea ice is lost. In the nudged simulations, the September sea ice edge does migrate towards the central Arctic. A substantial September sea ice cover is present in the nudged 1.5 and 2xCO_2 simulations September climatological sea ice state.

In both the nudged and the regular simulations, sea ice retreat occurs along the sea ice margin. Northward migration of the ice edge is not an unexpected response to a sudden increase incoming longwave radiation resulting from a CO_2 perturbation. In regions where the main surface energy balance in the control simulation is between outgoing longwave and incoming shortwave, a northward retreat of the ice edge leads to a new surface energy balance, because less shortwave radiation comes in throughout the year more Northward (Notz and Stroeve, 2016).

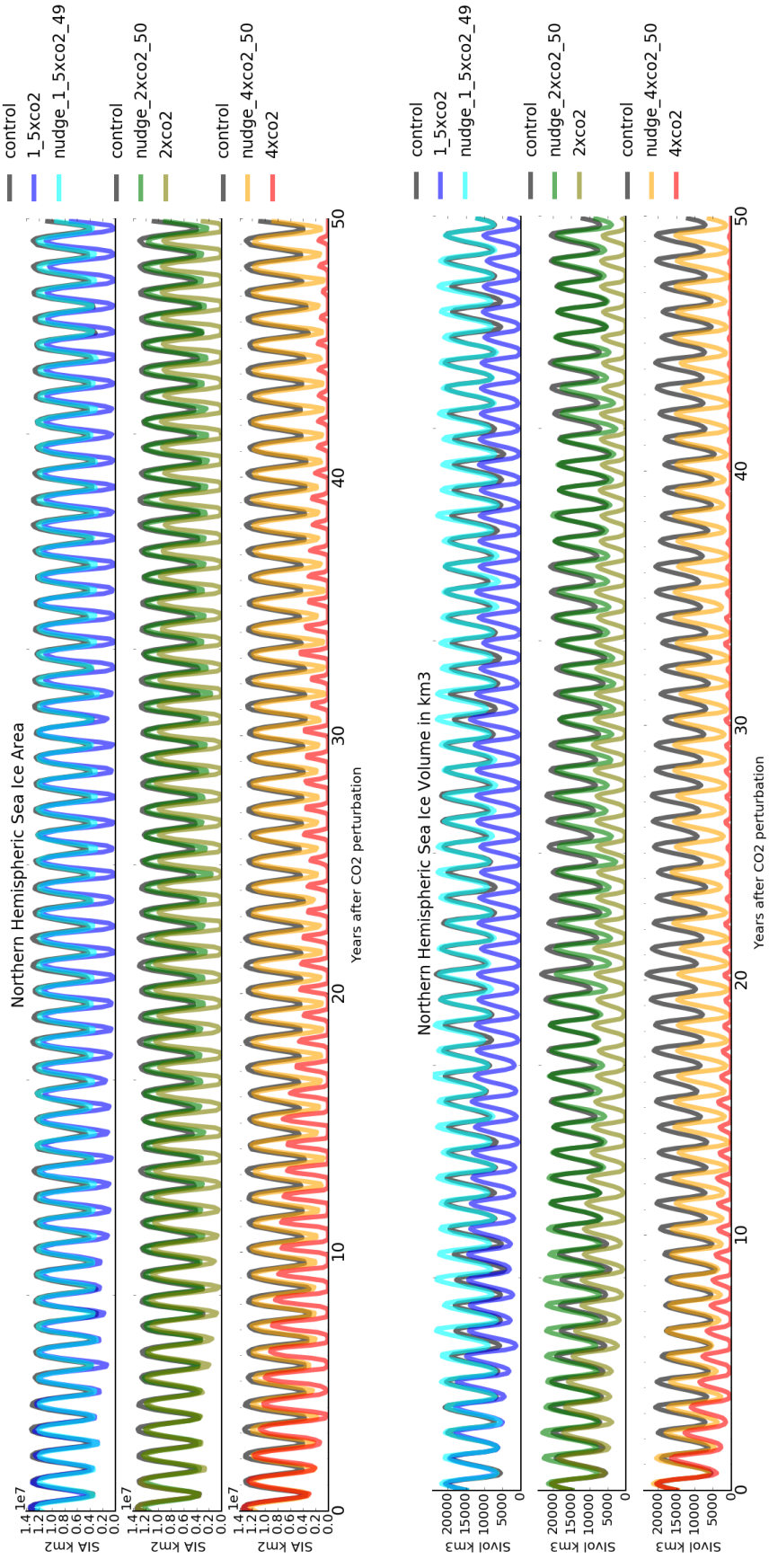

Figure 3: Time series of sea ice area (top) and sea ice volume (bottom) in the Arctic for each simulation. Blue lines represent 1.5xCO_2, green lines 2xCO_2 and red lines 4xCO_2.**Top**: Northern Hemispheric sea ice area. **Bottom**: Northern Hemispheric sea ice volume. In the regular CO_2 simulations sea ice starts to retreat immediately after the CO_2 perturbation whereas in the nudged simulations the sea ice stays close to the control simulation in the first years. Later in the simulation, winter sea ice stays closer to the control than summer sea ice.

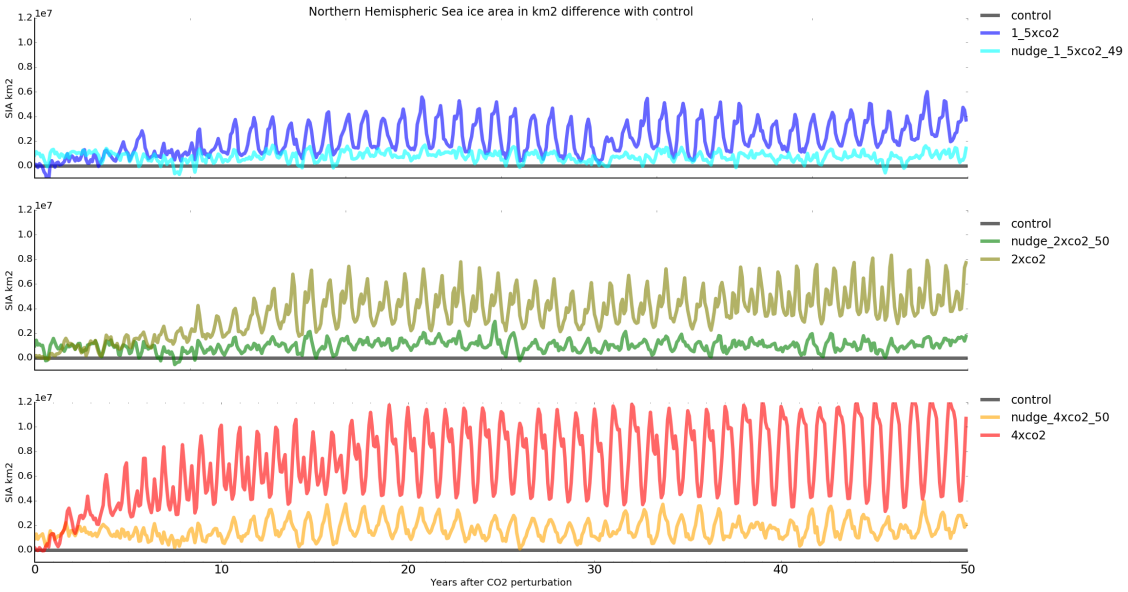

(a) Difference between the control and CO_2 simulations of total NH sea ice area in km^2

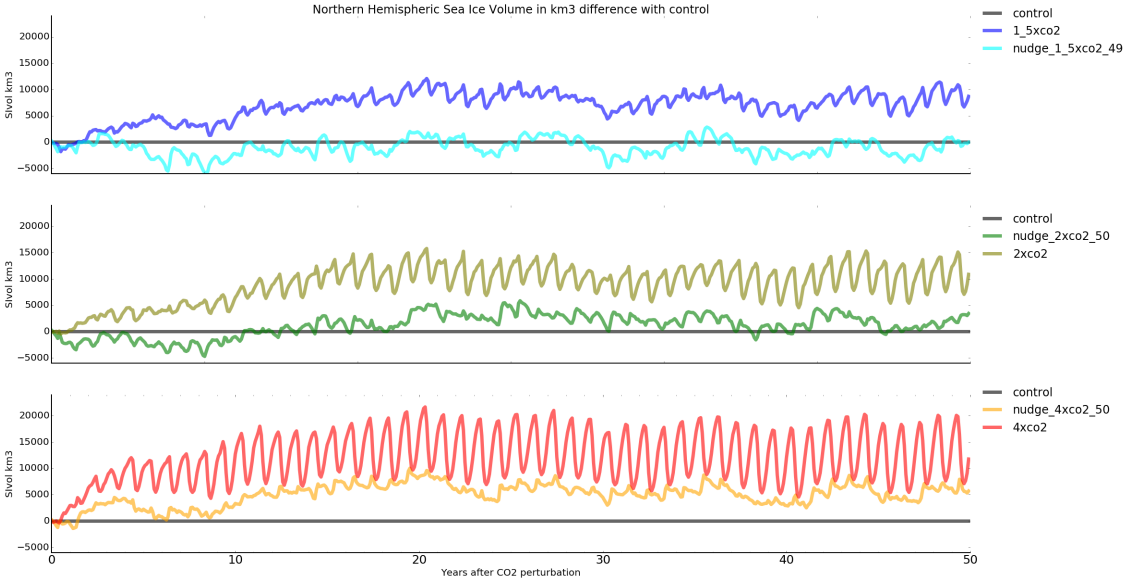

(b) Difference between the control and CO_2 simulations of total NH sea ice volume in km^3

Figure 4: Time series of total Northern hemispheric sea ice compared to the control simulation (forced simulation - control simulation). (Positive values indicate an ice loss, negative values indicate an ice gain in comparison with the control simulation).

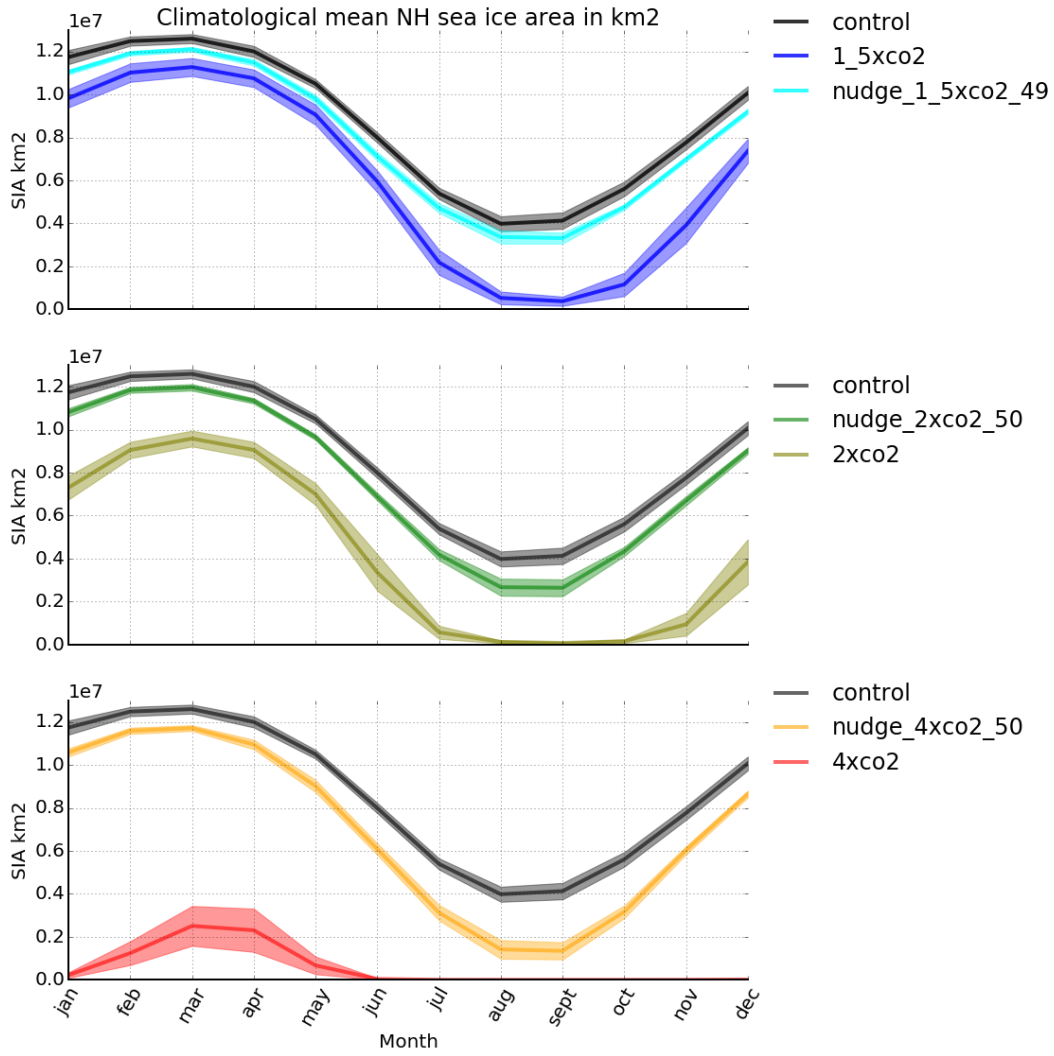

Figure 5: Climatological seasonal cycle of mean sea ice area in km^2 of the last 25 years of integration. The filled areas indicate one standard deviation of the 25 monthly values, which is a measure for the inter-annual variability of the seasonal cycle over these 25 years.

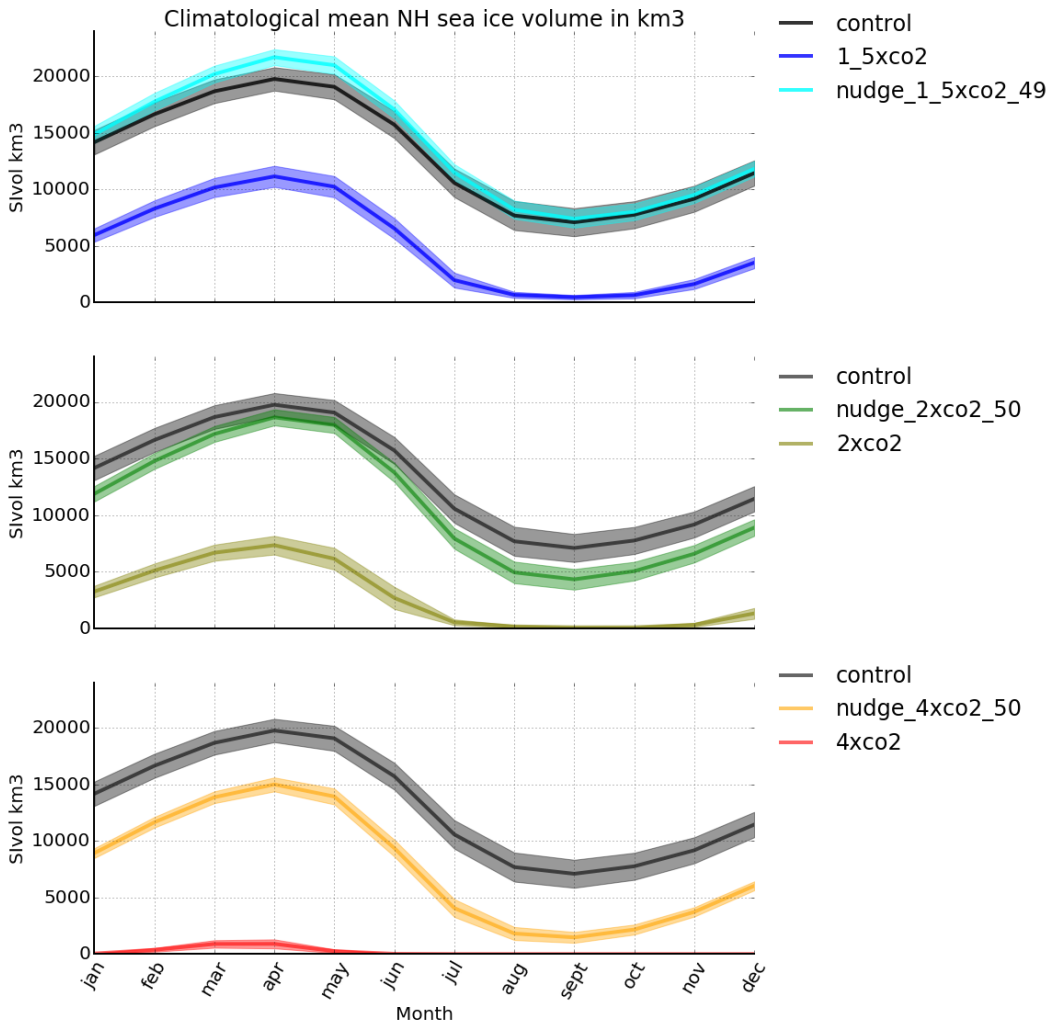

Figure 6: Climatological seasonal cycle of mean sea ice volume in km^3 of the last 25 years of integration. The filled areas indicate one standard deviation of the 25 monthly values, which is a measure for the inter-annual variability of the seasonal cycle over these 25 years.

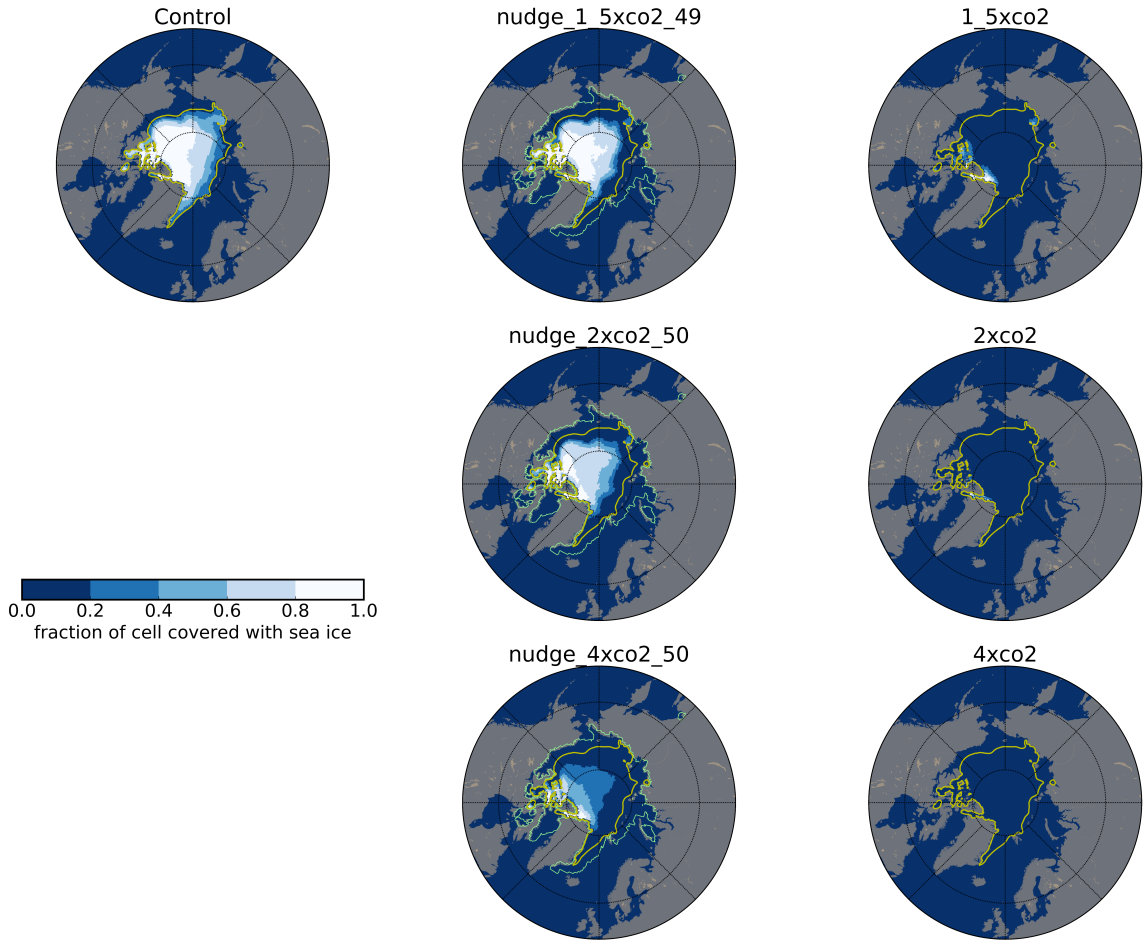

Figure 7: Climatological September mean sea ice concentration of the last 25 years of integration. The yellow line is the 0.15 sea ice concentration contour of the control climatology in September. The green line indicates the edge of the nudge mask.

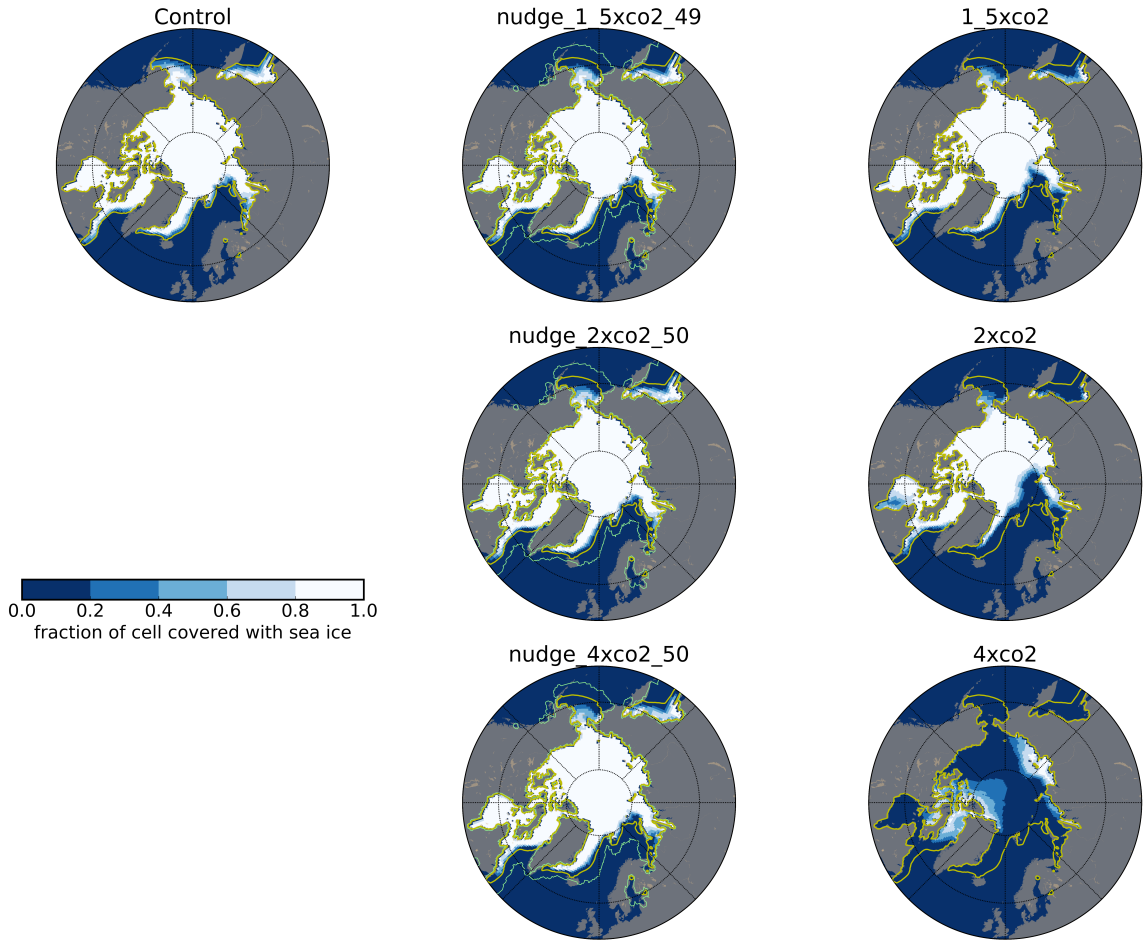

Figure 8: Climatological March mean sea ice concentration of the last 25 years of integration. The yellow line indicates the 0.15 sea ice concentration contour of the control climatology in March. The green line indicates the edge of the nudge mask

In the nudged simulations, 95% of the total PD mean March sea ice area is maintained (see Table 2) by the nudging. The March sea ice concentration distributions in the control and the nudged simulations (Fig. 8) look rather similar, except for a small retreat of the sea ice edge, resulting in a loss of 5% of the PD area. Also in the regular CO_2 simulations, the winter sea ice distribution of the last 25 years seems similar to the control distribution, except in the Barents sea and Nansen basin. In the current climate, most sea ice retreat occurs in these regions, according to satellite observations (Li et al., 2017).

In contrast to the regular simulations, no sea ice retreat occurs in the Barents Sea in the nudged simulations (Fig. 8). For this reason, our results suggest that the ocean plays an important role in sea ice retreat in the the Barents Sea, because by specifically nudging the ocean, the sea ice is preserved there. This is in line with findings from earlier studies, who found that the Barents Sea is a dominant region for total Arctic sea ice variability, and that the ocean heat flux is the dominant contributor to sea ice retreat in the Barents Sea (Årthun et al., 2012; Smedsrud et al., 2013; Li et al., 2017; van der Linden et al., 2017).

The sea ice retreat that occurs in September in the nudged simulations is already a large fraction of the total September sea ice (Table 2 and Fig 7). This illustrates that the nudging method is not able to avoid the emergence of a large fraction of open water areas in the central Arctic in summer. A general conclusion from Table 2 is that the larger the initial forcing due to CO_2 is, the less the nudging is able to maintain PD sea ice. Based on the summer ice loss, in the nudged 4xCO_2 simulation, we can conclude that our current nudging method is only able to to maintain PD sea ice if the radiative forcing is equal or smaller than that for 2xCO_2. The "unwanted" Arctic sea ice retreat compared to PD in the nudged simulations is not in accordance with the assumptions involved in evaluating the sea ice feedback in chapter 3. Hence, due to the mismatch of sea ice cover between the nudged and control simulations, the accuracy of our sea ice feedback estimate will decrease. The implications for the sea ice feedback estimate are elaborated on in more detail in the discussion section.

Interestingly, the nudging method leads to an increased sea ice thickness in the nudged 1.5xCO_2 simulations. The seasonal cycle (Fig. 6) of the sea ice volume shows that this is especially the case in winter. In the nudged 2xCO_2 simulation, the sea ice is also thicker during the first 10 years (Fig. 4b). This is likely due to the fact that salinity nudging applied the minimum rather than the mean. Also, nudging the Arctic Ocean field towards PD extreme negative salinity anomalies and mean temperature changed the ice volume inter-annual variability.This is confirmed by the fact that the volume standard deviation band of the control simulation is larger than of the nudged simulations. This decreased variability is expected, because generally, forcing a field into a prescribed mean state dampens the natural variability. The damping term in the ocean temperature and salinity tendency equations can reduce the variability of the ocean heat flux towards the bottom of the ice.

4.3 The energy associated with temperature damping

The amount of energy used to damp the Arctic Ocean is calculated in Watts for each model grid cell. To explore where most damping energy is required, we calculated column sums and divide these sums by the grid cell area. In this way, we obtain an estimate of the nudge energy flux per location. We show both the local nudge energy flux per grid cell, as well as the total nudge energy divided by global area. This first measure can locally distinguish regions of small or large nudge energy flux on an annual basis. The second measure indicates the energy loss/gain by nudging on the global energy balance.

The nudge energy flux is a measure for how much the Arctic Ocean temperature state deviates from the PD mean Arctic Ocean state. Hence, the nudge energy is not directly related to the sea ice itself, and should therefore not be interpreted as a corrective heat flux required to maintain sea ice in warmer conditions. Rather it can be taken as a measure of heat storage in the Arctic Ocean that would have occurred if the heat flux from the atmosphere and the ice into the ocean were not damped. Also, the ocean heat transport from lower latitudes into the Arctic basin is damped and added in the nudge energy term.

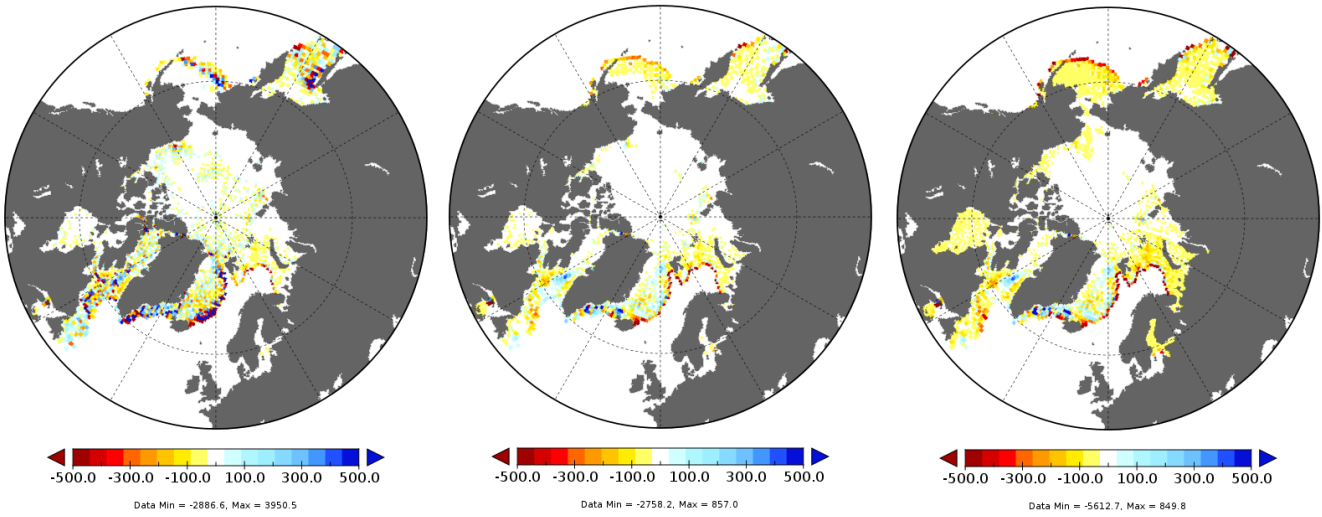

Figure 9: The vertically summed nudge energy averaged over the last 25 years of integration in Wm^{-2}. **Left:** nudge 1.5xCO_2 **Middle:** nudge 2xCO_2 **Right:** nudge 4xCO_2. The color bars are do not cover the full range of data values, minima and maxima are printed below the bars.Note that in the nudge 1.5xCO_2 simulation, the only the upper 200 meters are nudged.

4.3.1 A high magnitude nudge energy flux at the nudge mask edge

The spatial distribution of the annual mean (Fig. 9) shows that energy is mostly extracted at the edge of the nudge mask. More specifically, where the ice extent in the Arctic in the nudged simulation does not match with the ice extent of the control run, the local nudge energy flux is often larger than $\pm$ 1000 $W\ m^{-2}$. In other words, especially the outer cells of the nudge mask have extremely high nudge energy magnitude. These cells at the very edge, experience the advective ocean heat transport from neighboring, not nudged cells.

The way the nudge mask is constructed leads to enormous energy losses in regions where no sea ice present, that are nevertheless nudged towards the mean PD state. This means that we also nudge cells where sea ice occurred under extreme cold surface ocean conditions in the control simulation. Contrastingly, we nudge the ocean towards the mean temperature, thereby removing all ocean cold and warm extremes. As a consequence, we nudge the ocean towards mean temperatures, whereas under mean ocean temperatures sea ice would not grow in these cells. Hence, in these cells, heat exchange occurs between the ocean an the atmosphere, as there is no sea ice cover to insulate the ocean from the atmosphere. As a result, these cells will accumulate a large amount of heat in summer, which the nudging procedure directly tries to nudge away. hence, these gridcells accumulate a large nudge energy flux.

The large magnitude of energy loss flux at the edge of the nudge mask can further be attributed to the fact that nudging also occurs in sea ice export regions. In these regions, sea ice would not normally grow in the PD control situation. The amount of ice in export regions is mainly controlled by the winds and currents and to a lesser extent by ocean temperature and salinity. For this reason, the damping of the ocean salinity and temperature likely does not lead to growth of a sea ice cover, though is could slow down the melting of experted sea ice. Therefore, also cells in export regions accumulate a large nudge energy flux.

Generally, the nudging energy tendency distribution (Fig 9) exhibits an energy loss in most locations, as expected. However, around Greenland, the nudge energy can also be positive (blue), indicating that in the nudged simulations the ocean drifts towards to lower temperatures values than in the PD mean ocean state. The fact that the nudging procedure sometimes adds heat to the ocean is an unwanted side-effect of our nudging method. We conclude that there is still room for improvement as far as the nudging method goes. The discussion section contains several suggestions for improvements.

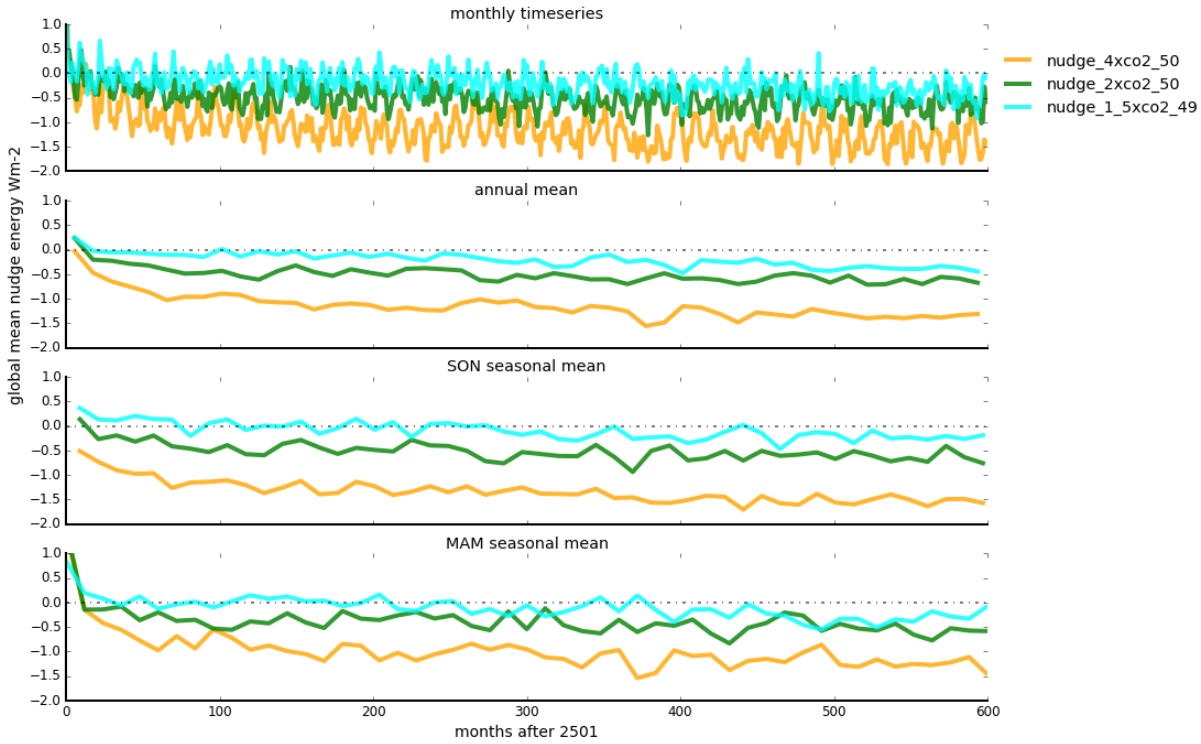

Figure 10: Time series of global average nudge energy flux in Wm^{-2}

4.3.2 The nudge energy flux in the global energy balance

The global nudge energy flux follows an exponential decrease with time (see Fig. 10). The fact that the initial nudge energy flux is positive, indicates the initial the Arctic Ocean is coincidently colder than the climatological mean temperature of the 60 year control simulation. The annual average nudge energy flux due to temperature damping in the last year of integration with (between parentheses the amount of initial radiative forcing due to CO_2) is: -0.44 (2.06), -0.67 (3.62) and -1.31 (7.69) $W\ m^{-2}$ for the nudged 1.5xCO_2, 2xCO_2 and 4xCO_2 simulations respectively (see Fig. 10(b)). Not unexpectedly, the larger the mismatch between the nudged simulation sea ice state and the control sea ice state, the more energy is required to restore the Arctic ocean to the control mean state.

The magnitude of the nudge energy exhibits a small seasonal cycle (Fig. 11). The amplitude of the seasonal cycle of nudge energy increases with increasing CO_2 perturbation strength. Restoring the Arctic Ocean towards the control equilibrium temperature requires most energy in summer, especially in august. Summer is also the season in which the nudged Arctic sea ice extent matches least well with the PD sea ice extent. The sea ice cover is thus a a very important insulator for the atmospheric heat to penetrate the ocean in summer.

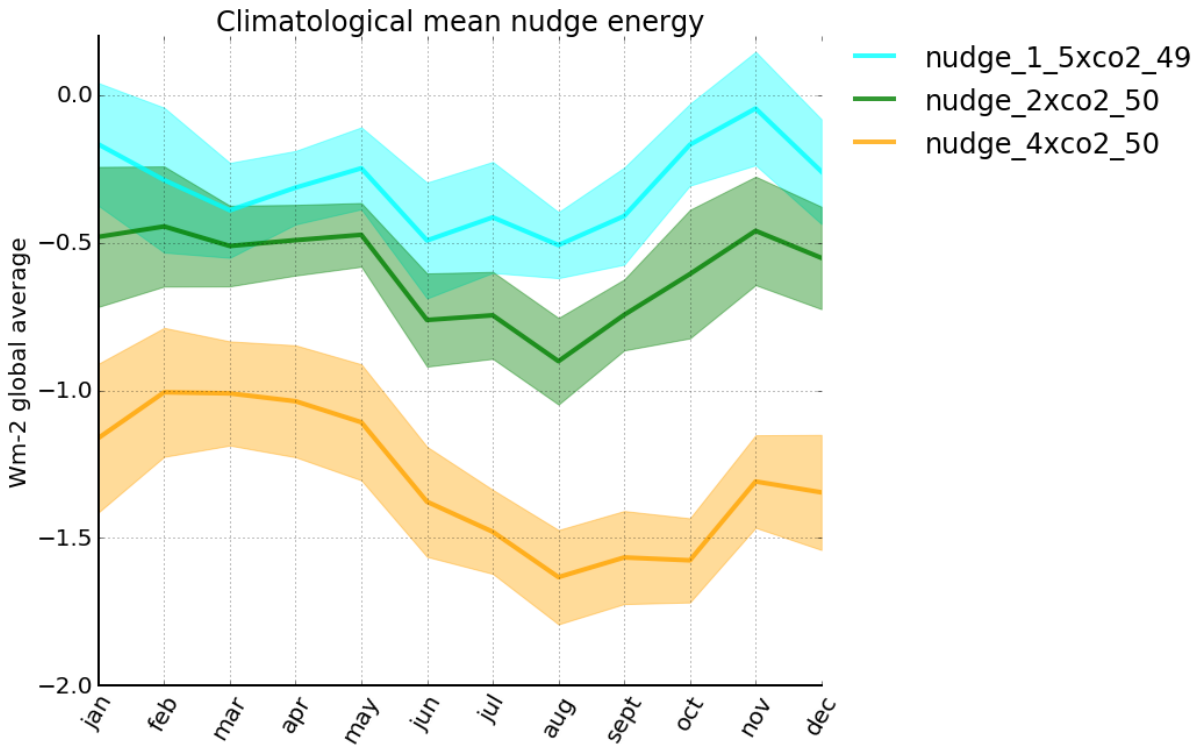

Figure 11: Climatological seasonal cycle of global mean nudge energy Wm^{-2} in the last 25 years of integration.

4.4 Climate and sea ice feedbacks

We compute the linear regression between the annual mean total net energy budget (Fig. 2(f)) and the annual mean global mean temperature response (Fig. 2(a)). The Y-intercept of the linear regression provides an estimate of the initial radiative forcing which is directly caused by the CO_2 perturbation (ΔQ in $W\ m^{-2}$) . The X-intercept of the linear regression yields of the equilibrium global mean surface temperature change (ΔT_s).

For the regular CO_2 simulations, the resulting estimates of ΔQ, ΔT and λ_f and error of the slope are presented in Fig. 12 and table 3. For the nudged simulations, the resulting estimates of $\Delta Q + \Delta E$, ΔT and λ_f and error of the slope are presented in Fig. 13 and table 4 . We only have one ensemble member per simulation, so the reported errors indicate the statistical uncertainty in the slope of the linear regression.

Table 3: Linear regression estimates between annual mean global mean TOA imbalance and surface air temperature,$R^{TOA} = \Delta Q + \lambda_f \Delta T$

Simulation	$\Delta Q\ Wm^{-2}$	ΔT_{eq} **K**	**slope** λ_f	**R value**
1.5xCO_2	2.06 $\pm$ 0.13	1.7	-1.22 $\pm$ 0.12	-0.83
2xCO_2	3.62 $\pm$ 0.14	3.08	-1.17 $\pm$ 0.07	-0.92
4xCO_2	7.69 $\pm$ 0.17	6.75	-1.14 $\pm$ 0.04	-0.97

We use the λ_f estimates from the nudged and regular simulation to compute the Arctic sea ice feedback (Table 5). The resulting estimates of the Arctic sea ice feedback are quite similar for all forcings. In general, the standard error of the estimate increases with increased initial forcing. This is because the climate response of the 4xCO_2 simulation is much larger than the climate

response in the 1.5CO_2 simulation. Hereafter, we argue that the 2xCO_2 simulations provide the most accurate estimate of the Arctic sea ice feedback strength.

The difference in global mean 2 meter temperature change between the nudged and the regular 1.5xCO_2 simulation is very small. Hence, a large part of the statistical uncertainly originates from

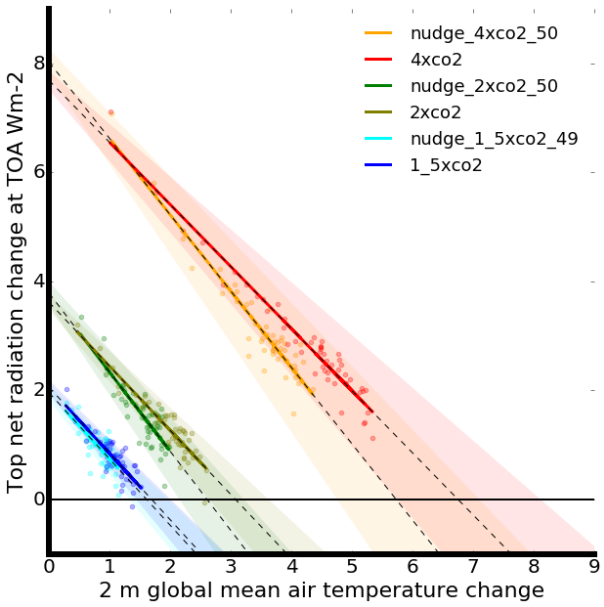

Figure 12: Linear regression between top net radiation imbalance and global mean 2 meter air temperature. The envelope the error due thestandard slope error and the standard intercept error.

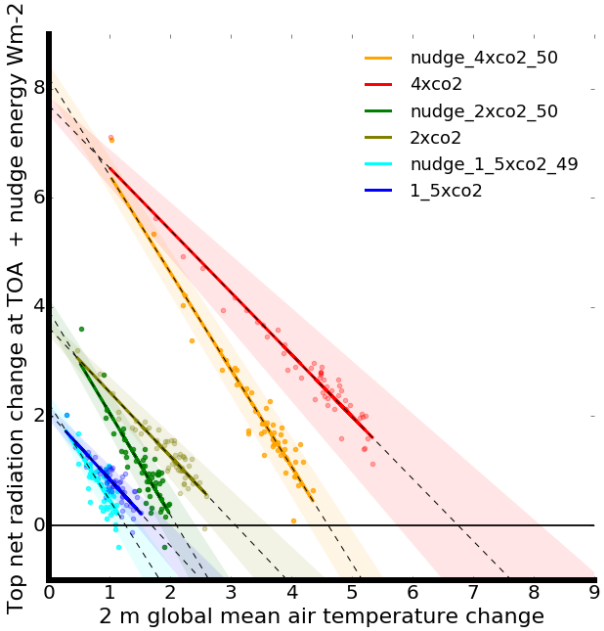

Figure 13: Linear regression between top net radiation imbalance and global mean nudge energy and global mean 2 meter air temperature. The envelope the error due thestandard slope error and the standard intercept error.

Table 4: Linear regression estimates of the nudged simulation global annual mean net TOA imbalance + global annual mean nudge energy against global mean temperature change. $\Delta R^{TOA} + E^{nudge} = \Delta Q + \lambda_f \Delta T$

Simulation	$\Delta Q + \Delta E$	ΔT_{eq}	**slope** λ_f	**R value**
nudge 1.5xCO_2	2.23 $\pm$ 0.17	1.26	-1.76 $\pm$ 0.19	-0.79
nudge 2xCO_2	3.92 $\pm$ 0.23	2.11	-1.86 $\pm$ 0.15	-0.87
nudge 4xCO_2	8.19 $\pm$ 0.26	4.68	-1.78 $\pm$ 0.07	-0.96

the inter annual variability. Furthermore, the estimate of the sea ice feedback in this simulation is likely largely influenced by the nudge energy, instead of the difference in sea ice feedback. Furthermore, none of the simulations resulted in a perfect match between in Arctic sea ice area and volume with the PD state. In the nudged 1.5xCO_2 simulation the winter sea ice is too thick compared to the control. The September sea ice loss in the 4xCO_2 simulation is quite large. Based on these caveats, we argue that the 2xCO_2 λ_{ice} provides the best estimate, since the various drawbacks are probably minimal: the large enough difference in climate response between nudged and regular simulations and an tolerable mismatch in nudged sea ice state compared to PD.

Table 5: **Estimates of the total Arctic sea ice feedback** λ_{ice}. The reported standard deviation represents the combined error of each linear regression.

Forcing	λ_{ice}
1.5xCO_2	0.55 $\pm$ 0.22
2xCO_2	0.68 $\pm$ 0.16
4xCO_2	0.63 $\pm$ 0.082

Having calculated the Arctic sea ice related feedback, we can this in context. Firstly, we compare our findings to the climate feedback parameters found in instantaneous CO_2 forced experiments from CMIP5 simulations (table 6). The sea ice feedback obtained from the 2xCO_2 simulations is 0.52 - 0.84 $W\ m^{-2}\ K^{-1}$. We expect the sea ice feedback to be positive, because the lapse rate and water vapor and albedo feedbacks are all positive in the Arctic. Our estimate ranged is not larger than the sum of all positive CMIP5 climate feedbacks, and the lower estimate is still in line with the ice-albedo only feedback. Although 0.68 is a large number for a feedback that is confined to the Arctic, which is only a fraction of the earth, it is not surprising that the Arctic contributes so heavily to the global climate sensitivity. The local feedback estimates from the kernel method surface albedo feedback and lapse rate feedback suggest large feedback strength in the Arctic locally (Block and Mauritsen, 2013) and they also interact strongly within the Arctic, such that they cannot be seen as linear additive feedbacks on global scale (Graversen et al., 2014). The range of 0.52-0.84 also falls reasonably well in the range of earlier estimates of the global sea ice temperature feedback evaluated by Bintanja and Oerlemans (1995).

While the range of our estimate is promising, we cannot generalize our estimate as it is based on only a single model. The amount of surface air temperature change in the Arctic locally depends to a large extent on the initial sea ice state (Van der Linden et al., 2014). In response to a transient 1% CO_2 increase per year starting from equilibrium 1850 conditions, models with initially more volume exhibit greater volume loss and a smaller sea ice area loss. Furthermore, Van der Linden et al. (2014) show that the sea ice in EC-Earth is comparatively thick in comparison with other models. Next, EC-Earth also has the third largest Arctic temperature trend and also the third largest Arctic winter temperature amplification of all CMIP5 models. This means that EC-Earth's sea ice feedback in response to a 1% CO2 increase is quite large in comparison with other models. In EC-Earth, the initially thickest ice leads to the third largest surface warming trend in the Arctic. This means that the Arctic in EC-earth is very sensitive to CO_2 perturbations, and that the sea

ice feedback estimate obtained with the nudging method in EC-earth might very well differ from other models. Applying our nudging method to other models would enhance the comparability of our Arctic sea ice feedback with other models.

Table 6: Climate feedback strengths ($Wm^{-2}K^{-1}$) from CMIP5 models from CO_2 doubling experiments, adapted from (Collins et al., 2013), their table 9.5. Total climate feedback parameter obtained using Gregory et al. (2004) from 23 models. Strength of the individual feedback from Vial et al. (2013) using the radiative Kernel method from Soden et al. (2008), obtained using 9 models. EC-Earth v 2.3 is not included in the ensemble. Our Arctic sea ice feedback estimate and range is in the right column.

	λ_{total}	λ_{Planck}	λ_{WV}	λ_{Γ}	λ_{α}	λ_{cloud}	λ_{ice}
Model mean	-1.1	-3.2	1.6	-0.6	0.3	0.3	0.68
90% uncertainty	±0.5	±0.1	±0.3	±0.4	±0.1	±0.7	0.52 to 0.84

In addition to these uncertainties, there are several limitation and caveats inherent to our method, mainly because the sea ice cover in the nudged simulations is not a perfect match with control simulation sea ice cycle. The nudged 1.5xCO_2 sea ice cycle resulted in too thick ice compared to the control, whereas in the nudged 2xCO_2 and 4xCO_2 simulations resulted in substantial summer sea ice area loss. The discussion section further elaborates on the consequences of the mismatch of control sea ice state and the nudged sea ice state for the sea ice feedback.

5 Discussion

Our estimate of Arctic sea ice feedback fits reasonably well in the CMIP5 global climate feedback estimates. However, our value is difficult to compare to other literature in which the spatial distribution of feedbacks and regional strength on the Arctic is studied. This is because our climate feedback estimate is a global feedback, while other studies explicitly compute the contribution of each feedback to Arctic warming (Hall, 2004; Graversen and Wang, 2009; Crook et al., 2011; Mauritsen et al., 2013; Graversen et al., 2014; Pithan and Mauritsen, 2014). Therefore, future analyses could include the application of the kernel method to our model results in order to differentiate the water vapor, cloud and albedo feedback contribution of Arctic sea ice individually. These types of analysis would aid the comparison of our results with other literature.

In this chapter we discuss further limitations and caveats of our feedback estimate. Furthermore we compare our nudging method to other methods from the literature that force the Arctic sea ice towards a prescribed state, including the energy correction terms used in these studies. Finally we present some ideas about how our nudging method can be improved.

5.1 The limitations of our Arctic sea ice feedback estimate

This subsection discusses various limitations of our feedback estimate. Firstly, the fact that our nudging method does not lead to a perfect match with the control PD sea ice state. Then we discuss the limits of the feedback calculation itself. Finally, we discuss a limitation of the climate model EC-Earth.

5.1.1 What are the implications of the mismatch between nudged and present-day sea ice state for the feedback estimate?

The way we compute the sea ice related feedback assumes that the Arctic sea ice state in the control simulation is similar to the Arctic sea ice state in the nudged simulations. However, our nudged simulations still include Arctic sea ice retreat in comparison with the control simulations, especially in summer (Table 2). Furthermore, the Arctic winter sea ice thickness is somewhat overestimated in the nudged 1.5xCO_2 and 2xCO_2 simulations (Fig. 6). These differences between the control and nudged sea ice states will add uncertainty to the sea ice feedback estimate. This uncertainty is larger in the case of a strong forcing, when the deviation in sea ice extent is largest. In the current method, there is no way to circumvent this issue. The only way to improve this

deficiency is by improving our nudging method in such a way that the sea ice is more accurately maintained.

The largest mismatch in sea ice cover between the nudged and the PD control simulations occurs in late summer and early autumn. Hence, our sea ice feedback estimate is likely not representative for the sea ice feedbacks that would follow a late summer and autumn sea ice retreat.

According to Crook et al. (2011), the main processes contributing to surface temperature amplification in the Arctic in autumn are the heat transport, storage and release from the ocean. As the mismatch in our nudged simulations is largest in autumn, we would expect that mainly this ocean heat storage process is under-represented in our sea ice feedback estimate. Normally (i.e. without nudging), an ocean temperature increase in summer would delay the growth of sea ice in the consecutive winter. However, this effect is not present in the nudged simulations, as the Arctic Ocean is nudged towards its PD state.

We argue that the error in our estimate of the Arctic sea-ice feedback due to the mismatch of September sea ice is relatively small, because the heat transport and storage effect of the sea ice related feedback is damped by the nudging of the ocean temperature. Consequently, in the regions of sea ice retreat in the nudged simulations, the winter surface temperature increase related to this ocean storage process is suppressed. In addition, the change in albedo feedback in late summer is limited, because the maximum surface albedo changes occur in spring. Furthermore, the reduction in sea ice albedo is largely masked by an increase in cloud albedo (Hall, 2004); hence, the effect of autumn sea ice changes in the nudged simulations on the net albedo feedback is limited.

Nonetheless, there will be a surface air temperature effect caused by the mismatch in the control and nudged sea ice state. This mismatch leads in the nudged simulations to an enhanced energy exchange between the atmosphere and the ocean. This heat exchange would not have occurred if sea ice cover was correctly nudged. It is not very straightforward to determine the net effect on the surface temperature in the regions of mismatch. If the nudging worked perfectly this would have two effects that oppose each other i) there would be no heat gain in the atmosphere in winter, because the heat exchange is blocked, and ii) there would not be a heat loss from the near-surface atmosphere to the ocean in the summer season. Hence, the mismatch likely has a seasonal imprint on the Arctic sea ice feedback, though we did not quantify the net effect on the feedback.

5.1.2 The role of changing ocean is not taken into account

Our estimate represents only the atmospheric part of the Arctic sea ice feedback. The melt of sea ice does not lead to a feedback on the ocean density in the nudged simulations, as a consequence of the nudging in the Arctic Ocean. Therefore, our estimate of λ_{ice} does not take into account the small positive feedback resulting from the ice-ocean interactions as described in section 2.3.

Another limitation of our method is related to the fact that nudging the Arctic Ocean potentially influences the ocean dynamics and ocean heat transport. Simply put, we force the Arctic Ocean into a colder state, but this colder water can also leak out of the Arctic though ocean currents. Hence, the application of the nudging method might have implications for ocean and sea surface temperatures outside of the Arctic. In section 3.3.1 we assumed that the ocean heat advection from the nudged regions to the rest of the global ocean change happens on such a long time scale that we can safely adapt the ocean structure below the ice, without disturbing the TOA radiative budget or surface temperature outside the Arctic. However, we did not verify this assumption. The change in the AMOC in the regular and nudged simulations could be compared to infer the influence of the nudging itself on changing ocean circulation. An assessment of the global surface ocean heat budget caused by the nudging is not so straightforward, and remains for now an open question.

We did not explicitly quantify the error in the Arctic sea ice feedback estimate. Therefore, the effect of these caveats on the Arctic sea ice feedback can only be discussed qualitatively. It is not straightforward whether the Arctic sea ice feedback strength would increase or decrease due to the mismatch between the PD and the nudged sea ice state. Overall, the loss of winter sea ice leads to stronger feedbacks than the loss of summer sea ice. As winter sea ice is preserved better

than September sea ice in the nudged simulations, the most important processes of Arctic sea ice induced feedbacks are probably assessed in our analysis of the feedbacks.

5.1.3 EC-Earth is not an energy conserving model

A disadvantage of using EC-Earth is that this model does not conserve energy in the coupled mode. The numerical advection scheme leads to a loss of atmospheric moisture. This means that water mass (thus latent heat energy) is lost in EC-earth, even if the net TOA radiative imbalance is zero. In the PD control equilibrium climate, this energy leak is -0.01 $W\ m^{-2}$, which seems negligible. However, we cannot be certain if this energy leak remains constant with changing climate. When atmospheric temperature increases, the water vapor content increases, leading to potentially more loss of atmospheric moisture in warmer climate simulations. A proper assessment of the energy leak magnitude in the new equilibrium could be obtained if the simulations would be allowed to equilibrate.

5.2 A comparison with other methods to fix the sea ice effect on climate in models

Recently, two studies used another methods to force Arctic sea ice in a prescribed state. We can compare their methods of keeping the sea ice at the desired state to our method. We can also compare the amount of energy required to obtain their sea ice states.

Deser et al. (2015) prescribe additional longwave radiative fluxes to the ice model at each grid cell if there is sea ice present in this grid cell. In order to obtain late twenty-first century sea ice comparable to PD sea ice in their simulation, they apply annually averaged 0.43 $W\ m^{-2}$ downward longwave radiation to the Arctic sea ice the CCSM4 model. Their longwave correction flux was seasonally varying but not spatially varying. This amount of radiative flux is about 6% of the total radiative forcing in the RCP8.5 scenario between 2000 and 2100 (6.7 $W\ m^{-2}$). Oudar et al. (2017) obtained preservation of 1970-2000 Arctic sea ice in a simulation under RCP 8.5 2085 radiative forcing. They use heat flux corrections in the non-solar heat flux of the ocean model (NEMO) specifically applied to model grid cells where $> 10\%$ sea ice retreat occurs between between the PD state and the RCP8.5 state. This means that they specifically anticipate the amount of energy required to maintain the sea ice. The amount of energy that was required to melt the Arctic sea ice into the RCP8.5 state starting from a PD climate was smaller that the energy required to grow PD Arctic sea ice into a RCP8.5 climate. Oudar et al. (2017) also emphasise that this discrepancy is related to the strong local feedbacks associated with the retreat of sea ice. We compare the amount of energy these studies use to establish their target sea ice during the simulations to the amount of energy we use damp the Arctic Ocean (Table 7).

Table 7: **Heat flux correction term in $W\ m^{-2}$ (global mean) to maintain sea ice in different studies**. Oudar et al. (2017) and Deser et al. (2015) use RCP 8.5 for future years. Note the different target sea ice states and higher radiative forcing (RF) than our study.

Simulation	model	start	end	Arctic sea ice target	RF	Annual mean	JAN	APR	AUG	OCT
ICE20 (Oudar et al., 2017)	CNRM-CM5	2085	2085	1970-1999	2085	-	-1.56	-0.61	-0.14	-0.79
ICE21 (Oudar et al., 2017)	CNRM-CM5	1985	1985	2070-2099	1985	-	1.3	0.51	0.11	0.66
ICE_coupled_20 (Deser et al., 2015)	CCSM4	2000	2000	1980 -1999	2000	-0.10	-	-	-	-
ICE_coupled_21 (Deser et al., 2015)	CCSM4	2000	2000	2080-2099	2000	0.43	-	-	-	-
nudge_2xCO_2_50 (this study)	EC-Earth	2000	2050	2000	2xCO_2 (3.62)	-0.59	-0.47	-0.49	-0.9	-0.6

The heat flux correction method of Oudar et al. (2017) works better than our nudging method to preserve PD sea ice in future radiative forcing circumstances. This is because they apply the heat correction specifically to regions were sea ice loss occurs and they fitted the amount of correction energy towards the expected amount of sea ice melt/growth. Also, their simulation set-up is fundamentally different. Their model simulations have constant radiative forcing at the initial and final state of their simulations, in which they push the sea ice into another state. Contrastingly, our simulations start from equilibrium without forcing, then apply instantaneous forcing and then we maintain the sea ice during integration while the climate system responds to the TOA imbalance applied. In contrast to our method, they need to apply the smallest energy correction in summer, and the largest in winter. This not surprising, because the Arctic amplification is strongest in winter.

5.3 Suggestions to improve the nudging technique

It is a promising result that the amount of energy that is lost in our ocean damping procedure is comparable or even slightly lower than the needed energy correction flux reported by Oudar et al. (2017). In our method, there is still room for improvement to reduce the amount of damping energy and to maintain more sea ice. In some locations, the current method leads in some locations to a net ocean temperature and salinity increase, which is an undesired effect.

Firstly, the method could be improved by allowing that the nudging to be applied only when this leads to freshening and/or cooling of the surface layer. Another common problem in our nudged simulations is that the salinity tendency damping often causes the model to crash. This is because the salinity tendency sometimes forces the salinity to become negative, which is of course unrealistic. Therefore, one perhaps should implement a separate damping timescale for temperature and for salinity. The optimal improvement would be to only nudge when it leads to cooling and freshening of the surface layer thereby maintaining a stable density stratification.

Secondly, we could reduce the amount of unnecessary damping energy by evaluating where sea ice growth occurs in the control simulation and nudge only there, instead of nudging all the areas where once there was sea ice present in PD. This would reduce the area where nudging would not lead to sea ice growth anyway. In this way, the export regions would be omitted from the nudge mask. Alternatively, the nudging procedure could be made dependent on the presence of sea ice during the integrations, but coding such a interactive nudging procedure is a complicated task.

Thirdly, the damping timescale could be reduced in deep ocean layers. The sea ice will not be directly influenced by the heat of the deep ocean layers. All these potential improvements would in theory reduce the total required nudge energy. Thereby, the influence of the nudge energy term in the total energy balance of the climate system will become smaller, and the influence of the nudging procedure on the sea ice feedback estimation would be reduced.

6 Summary and Conclusions

The retreat of Arctic sea ice invokes a cascade of climate feedback processes that contribute to the current global climate sensitivity. Climate feedback processes associated with the retreat of Arctic sea ice include changes the lapse-rate, cloud and surface albedo feedbacks, as well as changes in the rate of heat exchange between ocean and atmosphere. Changes in Arctic sea ice have consequences for climate on a global scale. This study is the first attempt to quantify the contribution of the Arctic sea ice to global climate sensitivity in the current climate.

To quantify the climate feedbacks associated with sea ice retreat, we compared the climate feedback of instantaneously CO_2 perturbed simulations starting from present-day (PD) to the climate feedback obtained from similar perturbed simulations, in which the Arctic sea ice is artificially kept close to its PD distribution. To this end, we built a nudging procedure in the ocean module (NEMO) of EC-Earth v2.3 and nudge the Arctic Ocean into its PD mean temperature and PD minimum salinity below the PD Arctic sea ice cover.We applied the new nudging method to instantaneously forced 1.5xCO_2, 2xCO_2 and 4xCO_2 simulations of 50 years. As a result, we were able to maintain about 95% PD mean March Arctic sea ice area in the last 25 years of all simulations. The summer sea ice cover was less well preserved - 80%, 64% and 32% of the PD September sea ice area was maintained in the nudged 1.5xCO_2, 2xCO_2 and 4xCO_2 simulations

respectively.

We estimated the Arctic sea ice feedback strength by subtracting the climate feedback estimate of the nudged simulation without sea ice retreat from the estimate of the regular simulations' climate feedback, making use of the Gregory method to estimate climate sensitivity. During the model integrations, we calculated the magnitude of the energy tendency correction associated with the nudging of temperature.

Taking into account our energy correction of the climate system, our best estimate of the Arctic sea ice feedback yields 0.68 $\pm$ 0.16 $W\ m^{-2}\ K^{-1}$, obtained from the CO_2-doubling simulation. However, the way this nudge energy flux should be taken into account to calculate the Arctic sea ice feedback remains a matter of interpretation. Our estimate of Arctic sea ice feedback fits reasonably well in earlier CMIP5 global climate feedback estimates and shows that the Arctic sea ice exerts a considerable effect to the global climate sensitivity.

While this estimate is promising, our method knows several limitations and caveats. The first caveat is that the nudged simulations still lose Arctic sea ice compared to PD, while we assume that the sea ice state in nudged simulations is equal to the PD sea ice state. Furthermore, our findings are based on only one simulation in EC-Earth, while it is known that the Arctic sea ice feedback strength is likely model-dependent. This estimate includes the Planck, lapse rate, cloud, water-vapor and albedo feedbacks related to Arctic sea ice. Our estimate shows that the Arctic sea ice makes a considerable contribution to the total climate sensitivity of EC-Earth (0.9 K $W^{-1}\ m^2$).

Further improvement of the nudging method is possible by minimizing the nudging in export regions, adapting the timescale of damping and applying nudging in a more sophisticated vertical distribution. In this way, the unwanted effects on the feedback estimate could be further reduced.

The fact that nudging the Arctic Ocean to a considerable extent enables us to keep the Arctic sea ice near its PD distribution suggests that the Arctic ocean salinity and temperature play an important role in the evolution of sea ice in the current climate. Future research concerning the evolution of Arctic sea ice towards future should therefore also consider the influence of the temperature and salinity structure below the sea ice.

What is happening below the Arctic sea ice does not stay below the Arctic sea ice.

References

Andrews, T., Gregory, J. M., Webb, M. J., and Taylor, K. E. (2012). Forcing, feedbacks and climate sensitivity in cmip5 coupled atmosphere-ocean climate models. *Geophysical Research Letters*, 39(9).

Andry, O., Bintanja, R., and Hazeleger, W. (2017). Time-dependent variations in the arctic's surface albedo feedback and the link to seasonality in sea ice. *Journal of Climate*, 30(1):393–410.

Årthun, M., Eldevik, T., Smedsrud, L. H., Skagseth, Ø., and Ingvaldsen, R. (2012). Quantifying the influence of atlantic heat on barents sea ice variability and retreat. *Journal of Climate*, 25(13):4736–4743.

Bintanja, R. and Oerlemans, J. (1995). The influence of the albedo-temperature feed-back on climate sensitivity. *Annals of Glaciology*, 21(1):353–360.

Block, K. and Mauritsen, T. (2013). Forcing and feedback in the mpi-esm-lr coupled model under abruptly quadrupled co2. *Journal of Advances in Modeling Earth Systems*, 5(4):676–691.

Bony, S., Colman, R., Kattsov, V. M., Allan, R. P., Bretherton, C. S., Dufresne, J.-L., Hall, A., Hallegatte, S., Holland, M. M., Ingram, W., et al. (2006). How well do we understand and evaluate climate change feedback processes? *Journal of Climate*, 19(15):3445–3482.

Bouillon, S., Maqueda, M. A. M., Legat, V., and Fichefet, T. (2009). An elastic–viscous–plastic sea ice model formulated on arakawa b and c grids. *Ocean Modelling*, 27(3):174–184.

Chung, E.-S. and Soden, B. J. (2015). An assessment of direct radiative forcing, radiative adjustments, and radiative feedbacks in coupled ocean–atmosphere models. *Journal of Climate*, 28(10):4152–4170.

Collins, M., Knutti, R., Arblaster, J., Dufresne, J.-L., Fichefet, T., Friedlingstein, P., Gao, X., Gutowski, W., Johns, T., Krinner, G., Shongwe, M., Tebaldi, C., Weaver, A., and Wehner, M. (2013). *Long-term Climate Change: Projections, Commitments and Irreversibility*, book section 12, page 1029–1136. Cambridge University Press, Cambridge, United Kingdom and New York, NY, USA.

Colman, R. A., Power, S. B., and McAvaney, B. J. (1997). Non-linear climate feedback analysis in an atmospheric general circulation model. *Climate Dynamics*, 13(10):717–731.

Council, N. R., Committee, C. R., et al. (2004). *Understanding climate change feedbacks*. National Academies Press.

Crook, J. and Forster, P. (2014). Comparison of surface albedo feedback in climate models and observations. *Geophysical Research Letters*, 41(5):1717–1723.

Crook, J. A., Forster, P. M., and Stuber, N. (2011). Spatial patterns of modeled climate feedback and contributions to temperature response and polar amplification. *Journal of Climate*, 24(14):3575–3592.

Deser, C., Tomas, R. A., and Sun, L. (2015). The role of ocean–atmosphere coupling in the zonal-mean atmospheric response to arctic sea ice loss. *Journal of Climate*, 28(6):2168–2186.

Fichefet, T. and Maqueda, M. (1997). Sensitivity of a global sea ice model to the treatment of ice thermodynamics and dynamics. *Journal of Geophysical Research: Oceans*, 102(C6):12609–12646.

Goosse, H. and Zunz, V. (2014). Decadal trends in the antarctic sea ice extent ultimately controlled by ice–ocean feedback. *The Cryosphere*, 8(2):453–470.

Graversen, R. G., Langen, P. L., and Mauritsen, T. (2014). Polar amplification in ccsm4: Contributions from the lapse rate and surface albedo feedbacks. *Journal of Climate*, 27(12):4433–4450.

Graversen, R. G. and Wang, M. (2009). Polar amplification in a coupled climate model with locked albedo. *Climate Dynamics*, 33(5):629–643.

Gregory, J., Ingram, W., Palmer, M., Jones, G., Stott, P., Thorpe, R., Lowe, J., Johns, T., and Williams, K. (2004). A new method for diagnosing radiative forcing and climate sensitivity. *Geophysical Research Letters*, 31(3).

Hall, A. (2004). The role of surface albedo feedback in climate. *Journal of Climate*, 17(7):1550–1568.

Hansen, J., Lacis, A., Rind, D., Russell, G., Stone, P., Fung, I., Ruedy, R., and Lerner, J. (1984). Climate sensitivity: Analysis of feedback mechanisms. *Climate processes and climate sensitivity*, pages 130–163.

Hazeleger, W., Wang, X., Severijns, C., Ştefănescu, S., Bintanja, R., Sterl, A., Wyser, K., Semmler, T., Yang, S., Van den Hurk, B., et al. (2012). Ec-earth v2. 2: description and validation of a new seamless earth system prediction model. *Climate dynamics*, 39(11):2611–2629.

Holland, M. M. and Bitz, C. M. (2003). Polar amplification of climate change in coupled models. *Climate Dynamics*, 21(3-4):221–232.

Koenigk, T., Brodeau, L., Graversen, R. G., Karlsson, J., Svensson, G., Tjernström, M., Willén, U., and Wyser, K. (2013). Arctic climate change in 21st century cmip5 simulations with ec-earth. *Climate Dynamics*, 40(11):2719–2743.

Langehaug, H. R., Geyer, F., Smedsrud, L. H., and Gao, Y. (2013). Arctic sea ice decline and ice export in the cmip5 historical simulations. *Ocean Modelling*, 71:114–126.

Li, D., Zhang, R., and Knutson, T. R. (2017). On the discrepancy between observed and cmip5 multi-model simulated barents sea winter sea ice decline. *Nature Communications*, 8.

Madec, G. et al. (2008). Nemo ocean engine.

Marotzke, J. (2000). Abrupt climate change and thermohaline circulation: Mechanisms and predictability. *Proceedings of the National Academy of Sciences*, 97(4):1347–1350.

Mauritsen, T., Graversen, R. G., Klocke, D., Langen, P. L., Stevens, B., and Tomassini, L. (2013). Climate feedback efficiency and synergy. *Climate Dynamics*, 41(9-10):2539–2554.

Notz, D. and Stroeve, J. (2016). Observed arctic sea-ice loss directly follows anthropogenic co2 emission. *Science*, 354(6313):747–750.

Oudar, T., Sanchez-Gomez, E., Chauvin, F., Cattiaux, J., Terray, L., and Cassou, C. (2017). Respective roles of direct ghg radiative forcing and induced arctic sea ice loss on the northern hemisphere atmospheric circulation. *Climate Dynamics*, pages 1–21.

Overland, J. E., Dethloff, K., Francis, J. A., Hall, R. J., Hanna, E., Kim, S.-J., Screen, J. A., Shepherd, T. G., and Vihma, T. (2016). Nonlinear response of mid-latitude weather to the changing arctic. *Nature Climate Change*, 6(11):992–999.

Pithan, F. and Mauritsen, T. (2014). Arctic amplification dominated by temperature feedbacks in contemporary climate models. *Nature Geoscience*, 7(3):181–184.

Screen, J. A. and Simmonds, I. (2010). The central role of diminishing sea ice in recent arctic temperature amplification. *Nature*, 464(7293):1334–1337.

Serreze, M. C. and Barry, R. G. (2011). Processes and impacts of arctic amplification: A research synthesis. *Global and Planetary Change*, 77(1):85–96.

Serreze, M. C. and Stroeve, J. (2015). Arctic sea ice trends, variability and implications for seasonal ice forecasting. *Phil. Trans. R. Soc. A*, 373(2045):20140159.

Shine, K. P., Cook, J., Highwood, E. J., and Joshi, M. M. (2003). An alternative to radiative forcing for estimating the relative importance of climate change mechanisms. *Geophysical Research Letters*, 30(20).

Smedsrud, L. H., Esau, I., Ingvaldsen, R. B., Eldevik, T., Haugan, P. M., Li, C., Lien, V. S., Olsen, A., Omar, A. M., Otterå, O. H., et al. (2013). The role of the barents sea in the arctic climate system. *Reviews of Geophysics*, 51(3):415–449.

Snape, T. J. and Forster, P. M. (2014). Decline of arctic sea ice: Evaluation and weighting of cmip5 projections. *Journal of Geophysical Research: Atmospheres*, 119(2):546–554.

Soden, B. J., Held, I. M., Colman, R., Shell, K. M., Kiehl, J. T., and Shields, C. A. (2008). Quantifying climate feedbacks using radiative kernels. *Journal of Climate*, 21(14):3504–3520.

Sterl, A., Bintanja, R., Brodeau, L., Gleeson, E., Koenigk, T., Schmith, T., Semmler, T., Severijns, C., Wyser, K., and Yang, S. (2012). A look at the ocean in the ec-earth climate model. *Climate Dynamics*, 39(11):2631–2657.

Stommel, H. (1961). Thermohaline convection with two stable regimes of flow. *Tellus*, 13(2):224–230.

Taylor, K. E., Stouffer, R. J., and Meehl, G. A. (2012). An overview of cmip5 and the experiment design. *Bulletin of the American Meteorological Society*, 93(4):485–498.

Valcke, S., Caubel, A., Declat, D., and Terray, L. (2003). Oasis3 ocean atmosphere sea ice soil user's guide. *Prisim project report*, 2.

van der Linden, E. (2016). *Arctic climate change and decadal variability*. PhD thesis, Wageningen University.

Van der Linden, E., Bintanja, R., Hazeleger, W., and Katsman, C. (2014). The role of the mean state of arctic sea ice on near-surface temperature trends. *Journal of Climate*, 27(8):2819–2841.

van der Linden, E. C., Bintanja, R., and Hazeleger, W. (2017). Arctic decadal variability in a warming world. *Journal of Geophysical Research: Atmospheres*.

Vial, J., Dufresne, J.-L., and Bony, S. (2013). On the interpretation of inter-model spread in cmip5 climate sensitivity estimates. *Climate Dynamics*, 41(11-12):3339–3362.

A Test phase of nudging technique development

We perform test simulations of 5 and 10 years to create a nudging method in the Arctic Ocean thats keep the Arctic sea ice close to its PD state under a changing climate. Therefore, we adapt the nudging routine $tradmp.F90$ in EC-earth ocean model NEMO for our specific goal. We tested different values for the inverse timescale of damping γ and different vertical extent of the nudge mask. Due to the nudging, the ocean model sometimes crashed.

In table 8 a summary of the test simulations and their resulting crashes or sea ice field is reported. Most crashes are related to the freezing point routine. Most likely, the salinity tendency term results in the $ocefzp.F90$ a forced root of a negative number. This error is referred to as ocfzp.pp.f90. Another common crash was an instability in the ocean model, when the CFL criterion was violated. This means that the ocean model horizontal velocities become too large. A reason could be that due to the damping, locally the gradient in temperature or salinity leads to instabilities. This error is referred to as CFL.

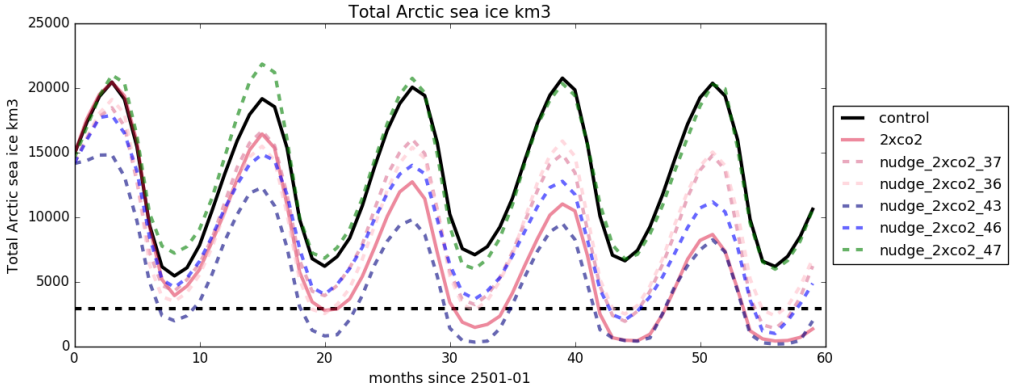

Figure 14: Example of sea ice volume in the 2xCO_2 test simulations. The nudge procedure was assumed to be sufficient if the total Arctic sea ice volume in the nudged simulations did not become smaller than the minimum sea ice volume that occured in the control simulation (black dotted line).

The test simulation of ID 47 with 2xCO_2 resulted in sufficient sea ice volume during a test simulation of 10 years (fig. 14). This version was used to perform the longer simulations of 50 years. Still this version did not lead to a stable simulation for all planned simulations (table 9), therefore only 3 out of the 6 planned long simulations are evaluated in the results.

Table 9: Planned long nudged simulations

Simulation name	CO_2	nudging type	nudging depth	yrs	result
nudge 1.5xCO_2_49	1.5x PD	damp mixed layer	upper 17 layers	50	used in results
nudge 1.5xCO_2_50	1.5x PD	damp whole column	42 layers	50	crashed after 13 years
nudge 2xCO_2_49	2x PD	damp mixed layer	upper 17 layers	50	crashed after 8 years
nudge 2xCO_2_50	2x PD	damp whole column	42 levels	50	used in results
nudge 4xCO_2_49	4x PD	damp mixed layer	upper 17 layers	50	crashed after 15 years
nudge 4xCO_2_50	4x PD	damp whole column	42 levels	50	used in results

Table 8: Test simulations and their results or crash report. This table summarises the different parameters that could be tuned in the nudging procedure. The ID refers to a combination of NEMO executable and EC-earth run script that was used. The sequence is not complete as some ID's refer to adaption of the run script that is not related to the nudging procedure. The amount of layers that is nudged in the vertical is reported in a sequence [upper level: lowest level]. The sea ice evolution in simulations that did not crash are reported as NS (not sufficient) or sufficient (S), which means that the amount of sea ice declined too much compared to PD. To illustrate this, some of the simulations total volume time series are presented in figure 14.

ID	CO_2	T_0	S_0	γ (days)	layers	Crash reason	Result	Note
27	4xPD	PD mean	PD mean	5	[2:42]	-	NS	surface layer not nudged
28	4xPD	PD mean	PD mean	1	[2:42]	-	NS	surface layer not nudged
29	4xPD	PD mean	PD mean	200^{-1}	[1:42]	ocfzpt.pp.f90	-	-
30	4xPD	PD mean	PD mean	100^{-1}	[1:42]	ocfzpt.pp.f90	-	-
31	4xPD	PD mean	PD mean	150^{-1}	[1:42]	ocfzpt.pp.f90	-	-
32	4xPD	PD mean	PD mean	1	[1:42]	ocfzpt.pp.f90	-	NS summer sea ice lost within first 5 years
33	4xPD	PD mean	PD mean	24^{-1}	[1:42]	ocfzpt.pp.f90	-	-
34	4xPD	PD mean	PD mean	12^{-1}	[1:42]	-	NS	-
35	4xPD	PD mean	PD mean	20^{-1}	[1:42]	-	NS	-
36	4xPD	PD mean	PD mean	20^{-1}	[1:17]	-	NS (fig.)	
37	2xPD	PD mean	PD mean	20^{-1}	[1:42]	-	NS (fig.)	
40	2xPD	PD mean	-	20^{-1}	[1:42]	CFL	-	nudge temperature only
42	2xPD	PD mean	PD mean	15^{-1}	[1:42]	ocfzpt.pp.f90	-	nudge temperature only
43	2xPD	-	PD mean	20^{-1}	[1:42]	-	NS (fig.)	nudge salinity only
44	2xPD	PD mean	-	30^{-1}	[1:42]	CFL	-	nudge temperature only
45	2xPD	PD mean	-	300^{-1}	[1:42]	CFL	-	nudge temperature only
46	2xPD	PD mean	PD mean*	20^{-1}	[1:42]	-	NS (fig.)	only nudge when it leads to sweetening
47	2xPD	PD mean	PD minimum	20^{-1}	[1:42]	-	S(fig)	used for long simulations
49	1.5xPD	PD mean	PD minimum	20^{-1}	[1:17]	-	S	50 years
49	2xPD	PD mean	PD minimum	20^{-1}	[1:17]	ocefzpt.pp.f90 year 13	-	-
49	4xPD	PD mean	PD minimum	20^{-1}	[1:17]	ocefzpt.pp.f90 year 15	-	-
50	1.5xPD	PD mean	PD minimum	20^{-1}	[1:42]	ocefzpt.pp.f90 year 8	-	restarting does not help, crashed
50	2xPD	PD mean	PD minimum	20^{-1}	[1:42]	CFL year 2 and 12	-	restart with centered differences continued for 50 years
50	4xPD	PD mean	PD minimum	20^{-1}	[1:42]	S	50 years	

B An Alternative approach to calculate the Arctic sea ice feedback

We estimated the Arctic sea ice feedback strength by subtracting the climate feedback estimate of the nudged simulation without sea ice retreat from the climate feedback estimate from the regular simulations, making use of the Gregory method to estimate climate sensitivity.

Furthermore, we assumed linear decomposition of the climate feedback parameter in a part related to Arctic sea ice melt and a remaining part.

$$\lambda_f = \lambda_{ice} + \lambda_{rest} \tag{17}$$

$$\lambda_f^{\mathrm{CO_2}regular} = \lambda_{ice} + \lambda_{rest} \tag{18}$$

$$\lambda_f^{\mathrm{CO_2}+nudge} = \lambda_{rest} \tag{19}$$

$$\lambda_{ice} = \lambda_f^{\mathrm{CO_2}} - \lambda_f^{\mathrm{CO_2}+nudge} \tag{20}$$

B.1 Energy balances

The Gregory linear regression technique is used to compute the equilibrium temperature response for instantaneous radiative, time-independent forcing. In the nudged simulations, we also include a non-radiative forcing which is state dependent. Therefore, the usage of the Gregory method is perhaps inappropriate to compute the climate feedback in the nudged simulations. This is the reason why we solve the energy balance in equilibrium explicitly to obtain the climate feedback estimate in the nudged simulation.

When we compare the nudged to the regular simulations, we aim to calculate the difference in response of the climate system to the changes in sea ice. In the nudged simulations, we add an extra energy term in comparison to the regular simulation. The main problem is that we only want we want to separate the climate feedback due to the changes in sea ice, rather than that we just measure how the climate responds differently because of the nudging itself. To this end, we evaluate the climate energy balance in each simulation, such that we explicitly take the nudge energy into account.

The energy balance in the regular simulations:

$$\Delta R = \Delta Q + \lambda_f \Delta T \tag{21}$$

For the regular simulations, the climate feedback estimate is straightforward. In equilibrium $\Delta R = 0$, so $\lambda_f^{\mathrm{CO_2}} = -\frac{\Delta Q}{\Delta T}$.

In the nudged CO_2 simulations, the climate is in equilibrium when the nudging energy is in balance with the imbalance at TOA. We call the magnitude of the nudge energy in equilibrium ΔE. We should carefully consider where to put ΔE in the energy balance equations (eq 21) in the nudged CO_2 simulations. We could see it as a forcing term or a response term of the climate.

The definition of what is to be considered a feedback and what to be considered as a forcing is proposed by (Gregory et al., 2004). "A practical distinction between a forcing and a feedback: Radiative forcing is a change in TOA imbalance brought about by the presence of the forcing agent, developing much more rapidly than the climate can respond (hence affecting the intercept of the regression line). A climate feedback is a change in TOA imbalance which arises from the climate response to the forcing (hence affecting the slope) [cf. (Shine et al., 2003)]."

In the end, it is a matter of interpretation if the nudge energy is seen as a forcing or a response of the climate system. Let us consider two cases. In the first case we put the nudge energy on the response side of the equation. In the second case, we put the nudge energy as a forcing term.

B.2 Case 1: ΔE = response

The CO_2 forcing is clearly developing more rapidly than the climate can respond, as it is put instantaneously. Also, the appliedCO_2-forcing does not depend on the climate state and is equally applied in the nudged and the regular simulation. The temperature damping term is not equally applied to the nudged and the regular simulation. One could regard the temperature damping term in the nudged simulations as a response to the applied forcing. If we would apply the temperature damping to the control simulation, this will not lead to a different climate state on the long term. Hence, this is an argument to regard the temperature damping term, thus ΔE as a response of the climate to the CO_2 forcing.

This is why we could see the nudging energy as a response term of the climate system, rather than a feedback or forcing term. As a consequence, we write the nudge energy flux in equilibrium on the left hand side of the total energy balance equation. Therefore we write the energy balance equation of the nudged CO_2 simulation in equilibrium:

$$\Delta R^{TOA} + \Delta E = \Delta Q^{\mathrm{CO_2}+nudge} + \lambda_f^{\mathrm{CO_2}+nudge} \Delta T^{\mathrm{CO_2}+nudge} = 0 \tag{22}$$

Here ΔE denotes the energy flux caused by the temperature damping term in the Arctic Ocean (the blue arrow in the upper right box of figure 1). Not all terms from this equation are known, because we do not run until equilibrium. Hence, we have no accurate estimate of $\Delta R^{TOA} + \Delta E$ in equilibrium. This is why we have to make an assumption:

In equilibrium:

$$\Delta E = \Delta Q^{\mathrm{CO_2}+nudge} + \lambda_f^{\mathrm{CO_2}+nudge} \Delta T_{eq}^{\mathrm{CO_2}+nudge} \tag{23}$$

We assume that the climate (λ_f) completely adjusted to the CO_2 perturbation. Note that this assumption is critical. Doing this, we see the remaining energy loss in the Arctic ocean (ΔE) as part of the response in equilibrium. In this interpretation of the energy balance, the new equilibrium global mean surface temperature present balance with the imbalance due to nudging. Hence, in nudged CO_2 simulations, we write the climate feedback (which does not include the sea ice feedback) as:

$$\lambda_{rest} = \frac{-\Delta Q^{\mathrm{CO_2}+nudge} + \Delta E}{\Delta T_s^{\mathrm{CO_2}+nudge}} \tag{24}$$

B.3 Case 2: ΔE = forcing

In the other case, we assume that the nudging forcing in equilibrium can also be seen as time independent. This assumption is quite illegitimate as the initial ice state would be much thicker and have a larger extend if all heat and salt correction would have been applied right at the start of the simulation. In balance, the TOA imbalance is then zero. We write the energy balance as:

$$\Delta R = \Delta Q^{\mathrm{CO_2}+nudge} + \Delta E_{eq} + \lambda_f^{\mathrm{CO_2}+nudge} \Delta T_{eq}^{\mathrm{CO_2}+nudge} = 0 \tag{25}$$

The estimate of $\lambda_f^{\mathrm{CO_2}+nudge}$ would then be:

$$\lambda_{rest} = -\frac{(\Delta Q^{\mathrm{CO_2}+nudge} + \Delta E)}{\Delta T_s^{\mathrm{CO_2}+nudge}} \tag{26}$$

This case 2 interpretation would only be valid if the climate system would be linear. It is however a brave assumption in a system that is known to generate strong feedback mechanisms.

B.4 Estimation of nudge energy in equilibrium

Our simulations do not extend until equilibrium is reached. Therefore, we must make an estimate of the nudge energy in an equilibrium situation. To this end, we obtain a linear fit function of the global mean nudge energy as function of global mean surface temperature change (table 10, similar to the linear regression method of Gregory et al. (2004). Based on the expected equilibrium temperature change that we obtain from the linear regression function between energy imbalance and global mean surface temperature increase, we make a best guess of the equilibrium nudge energy (ΔE(ΔT_{eq})).

The two cases to regard the nudge energy on the energy balance result in two different evaluations of the Arctic sea ice feedback:

Case 1: response

$$\lambda_{ice} = -\frac{\Delta Q^{\mathrm{CO_2}}}{\Delta T_s^{\mathrm{CO_2}}} - \frac{-\Delta Q^{\mathrm{CO_2}+nudge} + \Delta E_{response}}{\Delta T_s^{\mathrm{CO_2}+nudge}} \tag{27}$$

Case 2: forcing

$$\lambda_{ice} = -\frac{\Delta Q^{\mathrm{CO_2}}}{\Delta T_s^{\mathrm{CO_2}}} - \frac{-(\Delta Q^{\mathrm{CO_2}+nudge} + \Delta E_{forcing})}{\Delta T_s^{\mathrm{CO_2}+nudge}} \tag{28}$$

Table 10: Linear regression estimates between annual mean global mean nudge energy and surface air temperature, $E = a\Delta T + b$ The expected equilibrium temperature change is taken from table 4

Simulation	**linear E function**	**slope err.**	**R value**	**ΔE at T_{eq} in Wm^{-2}**
nudge 1.5xCO_2	$E = -0.55\Delta T + 0.49$	0.07	-0.78	-0.42
nudge 2xCO_2	$E = -0.41\Delta T + 0.33$	0.05	-0.79	-0.73
nudge 4xCO_2	$E = -0.37\Delta T + 0.45$	0.02	-0.93	-1.56

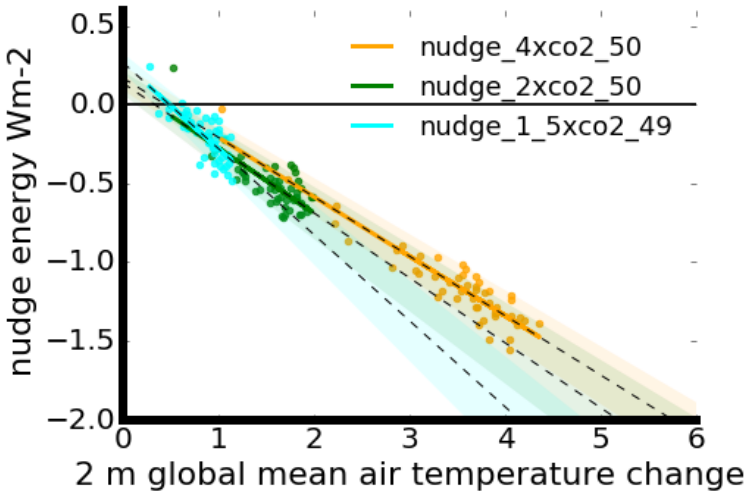

Figure 15: Linear regression between global mean nudge energy and global global mean 2 meter air temperature. These functions are used to compute the nudge energy associated with the equilibrium temperature change obtained from figure **??**.The envelope the error due thestandard slope error and the standard intercept error.

Table 11: **Estimates of** λ_{ice} obtained from three different methods. The difference in slopes as presented in the results section. Also the feedback estimated from solving energy balance as described in this appendix). The reported standard deviation represent the combined error of each linear regression used for the estimate

Forcing	difference in slopes Fig. 13	energy balance $\Delta E_{response}$	energy balance $\Delta E_{forcing}$
1.5xCO_2	0.55 ± 0.22	0.89 ± 0.34	0.27 ± 0.34
2xCO_2	0.68 ± 0.16	1.02 ± 0.30	0.34 ± 0.30
4xCO_2	0.63 ± 0.082	0.93 ± 0.35	0.22 ± 0.35

In table 11 the different estimates of the Arctic sea ice feedbacks are presented. All the possible estimates of the Arctic sea ice feedback estimates are constrained by the limitation of doing linear regressions to obtain the equilibrium temperature change in the nudged simulations. The only way to circumvent this issue is to run the simulations until equilibrium, when the nudge energy equals the TOA imbalance. The model is however subject to instabilities resulting in crashes when the ocean becomes unstable or when the salinities in the Arctic ocean are dampened to negative values. Besides, this is a very expensive computational task to run until full equilibrium which is not possible within the time given.

We did not present these alternative estimates in the results section as the assumptions required to write the energy balance equations are as illegitimate as using the usage of the Gregory method. Furthermore, the standard error of the λ_{ice} estimates in the energy balance method is higher than in the difference in slopes method. This is because we need to accumulate the errors from 3 linear regression, instead of two (like in the difference in slope method). All the possibilities to estimate the Arctic sea ice feedback in Table 11 are constrained by the limitation of applying linear regression to obtain the equilibrium temperature change in the nudged simulations. Therefore, the difference in slopes method seems to form the best estimate possible from our data.

Dankwoord

Dank aan Richard en Camiel dat ik dit zeer interessante project kon doen op het KNMI. Richard, bedankt voor je support en vertrouwen gedurende het project. Je zowel informele als temperende benadering waren erg prettig. Ik vond het heel tof dat ik de kans had om naar de EGU te gaan, daar heb ik erg veel van opstoken en het heeft me een hoop kansen geboden. Bedankt voor de schrijfsuggesties en adviezen voor de toekomst, beide hebben erg bijgedragen aan het feit dat ik na de zomer met veel plezier aan een PhD over zeeijs in Stockholm ga beginnen. Camiel, ik vond de balans tussen in het diepe gegooid worden en verhelderende suggesties uitstekend. Ik heb een hoop van je geleerd en ik vond het erg prettig met je samen te werken. Het was erg nuttig en leerzaam eens buiten de universiteit onderzoek te doen. Daarom bedank ik graag ook Willem Jan en Francesca voor het mogelijk maken van dit project. Zonder de vlotte start dankzij Frank had ik waarschijnlijk wat langer geworsteld met EC-Earth, bedankt!. Ik vind je zen benadering naar je werk erg bewonderingswaardig en ik hoop dat ik dat ook eens onder de knie krijg. The PhD thesis van Eveline kwam goed van pas en ik wil je ook graag bedanken voor het stellen van de juist vragen op het juiste moment.

Natuurlijk waren de dagen op het KNMI extra leuk door Sem en Jaro, wat een toffe collega master studenten. Ik vond het erg aangenaam met jullie op een kamer, voor zowel de fysieke als geestelijke fitheid. Daily life at KNMI was very enjoyable thanks to the nice colleagues that were always eager to help or in for a nice discussion. Thank you Philippe, Karin, Andreas, Dewi, Rein, Hylke, Marieke, Former, Jonathan, Geert-Jan, Jessica, Anna Lena, Anja and Kai. Rune Graversen, thank you for the very good discussions and interesting conversation.